THE CRYSTAL STRUCTURES OF SOME PHASES OF SILICA

by

WAYNE A. DOLLASE

B.S., University of Wisconsin
(1960)

M.S., University of Wisconsin
(1961)

SUBMITTED IN PARTIAL FULFILLMENT

OF THE REQUIREMENTS FOR THE

DEGREE OF DOCTOR OF

PHILOSOPHY

at the

MASSACHUSETTS INSTITUTE OF TECHNOLOGY

May 13, 1966

Signature of Author . . . .
Department of Geology and Geophysics

Certified by . . . .
Thesis Supervisor

Accepted by . . . .
Chairman, Departmental Committee
on Graduate Students

The crystal structures of some phases of silica.

by

Wayne A. Dollase

New crystallographic and structural data are presented
on four polymorphs of silica. A refinement of low cristo-
balite, which required correction of the data for the effects
of twinning, has confirmed Nieuwenkamp's proposed structure.
The refined Si-O distances are 1.601 and 1.608 $\mathring{A}$, both ±
.004 $\mathring{A}$. The intertetrahedral angle, Si-O-Si, is 146.8°
± 0.3°.

Tridymite from the Steinbach and two other meteor-
ites, and from a silica brick, has an apparent 30 x 49 $\mathring{A}$
pseudohexagonal cell at room temperature. This cell is
shown to be the twin composite cell, the true cell being
monoclinic C2/c or Cc with $a = 18.54$, $b = 4.99$, $c = 23.83$ $\mathring{A}$
and $\beta = 105.65^{\circ}$, $Z = 48$ SiO_2. The six individuals of the
twin are related by a six-fold twin axis parallel to [201]
of the monoclinic cell.

Above about 107° C the Steinbach tridymite transforms
reversibly to transitional tridymite which is identified
by a characteristic dynamic superstructure. The supercell
translation of this superstructure decreases continuously
from about 105 $\mathring{A}$ to about 65 $\mathring{A}$ as the temperature is raised
from 107° to 180° C. This behavior is similar to that ob-
served at the ferroelectric transition in $NaNO_2$.

At about 180° C the Steinbach tridymite transforms
reversibly to a third phase, namely, orthorhombic high
tridymite, which exists at least up to 250° C. In this
temperature range the space group is $C222_1$ with $a = 8.74$,
$b = 5.05$, and $c = 8.24$ $\mathring{A}$. A crystal structure determina-
tion has shown regular tetrahedra connected as in the Gibbs
ideal high tridymite structure. The lowering of the sym-
metry is brought about by a twisting of the tetrahedra
relative to each other. The average tetrahedral distance,
uncorrected for thermal motion, is 1.56 $\mathring{A}$. The rms ampli-
tudes of thermal vibration of the oxygen atoms normal to
the Si-O bonds are as high as 0.4 $\mathring{A}$ which partly accounts
for the apparent short Si-O distances.

The transitional tridymite subcell shows monoclinic P2$_1$ symmetry. A refinement based upon the substructure reflections only, has given nearly the same positional and thermal parameters as found for orthorhombic high tridymite. The only statistically significant deviations from the higher symmetry are very small shifts of the silicon atoms.

Thesis Superviser: Martin J. Buerger

Title: Institute Professor

Table of Contents

Chapter I

Background and plan of thesis

The problem

The silica system, composed of the polymorphous forms of SiO_2, is perhaps the most fundamentally important system in mineralogy. As an end member of all silicate systems, its structures and properties form a norm against which the parameters of a multicomponent silicate system may be compared. In their own right, most of the phases of silica occur naturally, some in great abundance. Furthermore, the structures of many of the phases have been adopted by other silicates and non-silicates thus forming an extensive family of derivative structures. Finally, due to the large number of different structure types displayed by this one compound, it has become a model and type case in the study of polymorphic transformations.

For all these reasons it might be expected that silica would be one of the most studied of chemical compounds; and that its crystal structures would be among the best known. The two very recent volumes of Frondel (1962) and of Sosman (1965), each devoted entirely to this compound, show the large amount of work that has been done. It is, however, somewhat surprising to find that although the general framework of each of the silica structures is

believed known, their exact structures are poorly known
or entirely unknown. In fact, the only silica structure
which is well known by modern standards is that of low
quartz. The symmetries and locations of some of the atoms
in high quartz are disputed. The entire tridymite group
is unknown except for the original very rough qualitative
structure proposed by Gibbs. Different investigators
have proposed different symmetries and structures for the
cristobalites, both high and low. The symmetry of coesite
is at least open to question. The structure has not been
refined and the proposed symmetry constrains a Si-O-Si bond
to be 180°, (the existence of such bonds, at room temperature,
has not been well authenticated, and is doubted by some
authors). Lastly, as pointed out by Wyckoff (1963), the
published structure of keatite leads to SiO_4 tetrahedron
with three bonds of normal length (ca. 1.6 $\overset{o}{A}$) and a fourth
bond of 3.7 $\overset{o}{A}$. This is almost surely incorrect.

The reasons for these uncertainies are two-fold:
the difficulty of obtaining good single-crystal intensity
data, and the difficulty in determining the true symmetries.
The first problem stems from the frequent lack of good
single crystals, the apparent ubiquitous twinning of every
one of the phases, and in some cases the occurrence of a
weak superstructure. The second problem is due also to the
twinning and to the fact that the required symmetry is
expressed only by relatively small deviations from a strong

pseudosymmetry. The lack of knowledge of the true symmetry does not prevent the determination of the general mode of tetrahedral linkage, but does prevent the determination of the details, namely the bond distances and angles, the rotations, tilting, or distortions of the tetrahedra, the thermal vibrations, etc., all of which are dictated or strongly restricted by the symmetry.

Scope of the thesis

Because of the importance of the system and because of its crystallographic complexity, the silica system poses an interesting problem. A crystallographic re-study of the system was, therefore, undertaken, and the first group of new results comprises this thesis. The individual topics, insofar as they are separable, are treated in the five succeeding chapters and an appendix. The second chapter is concerned with the structure of cristobalite at room temperature. A procedure had to be developed to obtain the true structure factors from the superposed diffraction data measurable from twinned material. Once this was done the refinement, confirming an earlier structure proposal, proceeded smoothly.

The largest unknown segment of the silica system, the tridymite group, was then studied. The first result was the establishment of the existence of at least two fundamentally different tridymites. The tridymite of ceramic silica brick and of meteorites is distinctly different from

all presently known natural, terrestrial tridymites. The symmetry and twinning of the first type are reported in Chapter 3. The next chapter describes the most unexpected finding of the study, a remarkable dynamic superstructure which seems to occur in all tridymites at their high-low transformation. This superstructure shows a temperature-dependent translation that changes continuously from about 60 Å to over 100 Å, as the temperature is raised through a 70° C interval. The superstructure appears to be due to an ordering of thermal vibrations in the form of waves, and is only the second reported example of this phenomenon, and the first known example in a mineral. Similar superstructures may be a general accompaniment to such transformations.

Chapters 5 and 6 report complete crystal-structure determinations of tridymite from the Steinbach meteorite in two different structural states, at 220° C and at 120° C. Both structures are found to be related to the ideal high tridymite structure by slightly different distortions. The unusually large thermal vibrations found for the oxygen atoms, even at as low a temperature as 120° C, help explain the behavior of the tridymite group.

The appendix describes the construction and operation of the furnace used in making most of the x-ray diffraction measurements above room temperature. This furnace was specifically designed for the single-crystal counter diffractometer, and represents several improvements over previous designs.

It was hoped at the outset that an intensive study restricted to a few of the phases of this system would point out the general procedures required in the eventual solution of all of the structures. This hope is now believed to have materialized. The main crystallographic obstacles standing in the way of solution of this group of structures have been overcome. The procedure for obtaining the structure factors from twinned crystals should have application in most of the other structure solutions. The single-crystal counter diffractometer has been shown to be capable of determining the small deviations in symmetry that occur in this system provided proper precautions are observed. And finally, the insight gained from the present structural studies should prove valuable in deciding what to look for and how to interpret what is observed in the studies of the remaining phases of silica.

Clifford Frondel (1962), The system of mineralogy, 7th ed.,
    vol. III: Silica minerals. John Wiley and Sons,
    New York, New York.

Robert B. Sosman (1965), The phases of silica, Rutger
    University Press, New Brunswick, New Jersey.

Ralph W. G. Wyckoff (1963), Crystal structures, 2nd ed.,
    vol. I, Interscience Publishers, New York, New York.

Chapter II

Reinvestigation of the structure of low cristobalite

Abstract

Twinned crystals of low cristobalite from Ellora, Hyderabad, India were found to have space group $P4_12_1$ (or $P4_32_1$) and cell dimensions $a = 4.97_8$ and $c = 6.94_8$ Å. A three-dimensional full-matrix least-squares refinement based upon 110 integrated intensities which were corrected for the effects of twinning, confirmed Nieuwenkamp's original structure and reduced the final R value to 4.4%. The refined set of four positional parameters are; $u = .30004 \pm .00033$, $x = .23976 \pm .00089$, $y = .10324 \pm .00085$, $z = .17844 \pm .00052$. These refined parameters lead to Si-O distances of $1.601 \pm .004$ and $1.608 \pm .004$ Å.

Introduction

High cristobalite is the polymorph of SiO_2 whose stability range occurs between 1470° and the melting point of 1728°. Upon cooling, it tends to exist metastably down to a variable inversion temperature of about 268° where it inverts to low cristobalite. The exact structures of the cristobalites are necessary to the understanding of the silica system, silica polymorphism, and the large field of silicates having related structures. Accordingly, the cristobalite structures have received considerably attention. Besides the early direct crystal-structure determinations, which are reviewed below, there have been a number of later, less direct studies which have yielded structural implications. The results of this latter group have been included, in the main, in the recent compilation of Frondel (1962).

Previous structural studies

The first structural study of high cristobalite was made by R. W. G. Wyckoff (1925) using powder photographs taken at 290° and 430°. The proposed structure belonged to the isometric space group Fd3m. The agreement between the 16 observed and calculated intensities, some of which were the sum of superposed powder lines, was fair, and could be improved somewhat by increasing the scattering power of the silicon atom relative to that of the oxygen atom. This structure, as well as all following cristobalite-structure proposals, showed an infinite three-dimensional

network of more or less regular SiO_4 tetrahedra with all corners shared. The silicon-oxygen distance in Wyckoff's structure was 1.54 A and the Si-O-Si angle between joined tetrahedra was $180°$.

Tom F. W. Barth (1932a) suggested a high-cristobalite structure belonging to space group $P2_13$ on the basis of some extra lines in the powder photographs (taken at temperatures up to $500°$) which are not allowed by Wyckoff's space group. The agreement between the 17 observed and calculated intensities was rather poor. Two-thirds of the intensities actually observed were the sums of two or more nonequivalent reflections. The Si-O distances ranged from 1.58 to 1.69 A.

Later in the same year Barth (1932b) made the first structural study of low cristobalite. Reasoning that it must belong to a subgroup of $P2_13$, and ruling out, on optical grounds, systems more symmetrical than orthorhombic, he arrived at space group $P2_12_12$. With this space group and with the pseudoisometric cell dimensions, nearly all the lines of the powder photographs he used were the sums of two or three nonequivalent reflections. The agreement between the 13 observed and calculated intensities was fair. The Si-O distances for this model ranged from 1.50 to 1.75 A.

W. Nieuwenkamp (1935) reinvestigated low cristobalite and suggested a structure belonging to the tetragonal space group $P4_12_1$. The structure determination was made by

qualitative estimation of intensities from rotation photographs made with twinned material. Due to the fortuitous cell dimensions many of the reflections were superposed on the photographs making it possible to estimate only the combined intensities of these pairs. The two Si-O distances of this model were both 1.59 A, and the Si-O-Si angle was 146°.

Nieuwenkamp (1937) also reinvestigated high cristobalite and proposed a third structure. From rotation photographs taken at 270°, using the same crystals as in the low-cristobalite study, he determined the space group to be Fd3m, the same as that proposed by Wyckoff. The best fit of the 25 observed and calculated intensities was with the oxygen atom disordered around the circumference of a circle of radius 0.4 A. This circle was oriented normal to the Si-Si axis of joined tetrahedr. Nieuwenkamp's model gave fair agreement of intensities and could account for Wyckoff's observation of the low scattering power of the oxygen atom. The Si-O distance in this model was 1.59 A and the Si-O-Si angle was 151°.

On the basis of these several structure determinations, which are characterized by meager, ambiguous data leading to conflicting results, the structures of the cristobalites are, at best, somewhat uncertain and merit reinvestigation. It is the purpose of this paper to report the results of the reinvestigation of the low-cristobalite structure.

Unit cell and space group

Crystals of low cristobalite from Ellora, Hyderabad, India were kindly made available from the Harvard Museum collection by Professor Clifford Frondel. A description of the material from this locality is given by Frondel (1962, page 282), and by Valkenburg and Buie (1945).

The cell dimensions and systematic absences were determined from precession photographs, taken into account the twinning which is discussed below. The diffraction symbol is $4/mmmP4_1/-2_1-$, which determines the space group as $P4_12_1$ or its enantiomorph, $P4_32_1$. The cell dimensions, $a = 4.97_8$ and $c = 6.94_8$ A, compare well with the values given by Frondel (1962, page 276).

When dealing with a primitive tetragonal lattice it is possible, though unconventional to choose a C - centered cell. The relationship between the two cells is shown in Fig. 1$\underline{A}$. For the particular case of low cristobalite this C - centered cell is pseudoisometric. The discrepancy between the c-axis translation and t_{110} $(=\underline{a} \, 2)$ of the primitive cell, is only 1.3%. This pseudoisometric cell is dimensionally equivalent to the high-cristobalite cell.

Description of the twinning

X-ray examination of the few available crystals from this locality showed that each of them was twinned. The pattern of reflections given by c-axis precession photographs is illustrated in Fig. 2$\underline{A}$. Besides the reflections attributable to the $P4_12_1$ cell described by Nieuwenkamp

a)

b)

Fig. 1

a)

b)
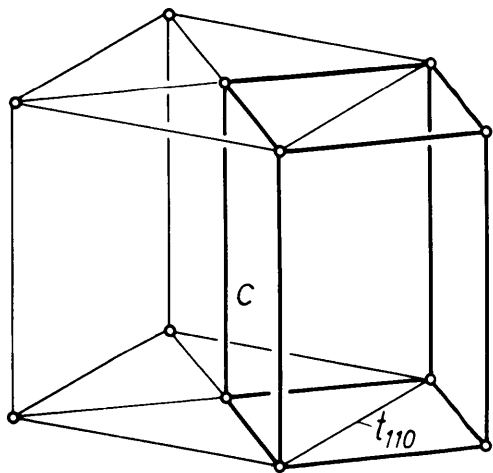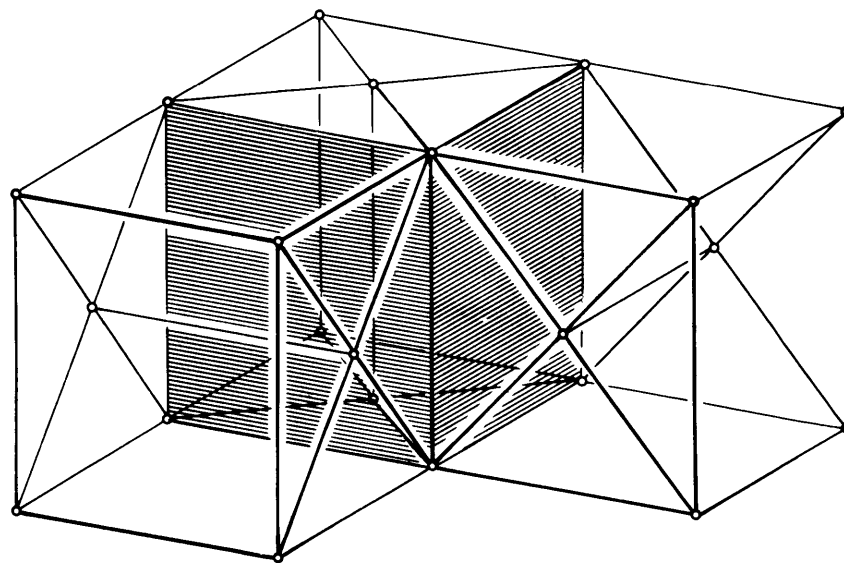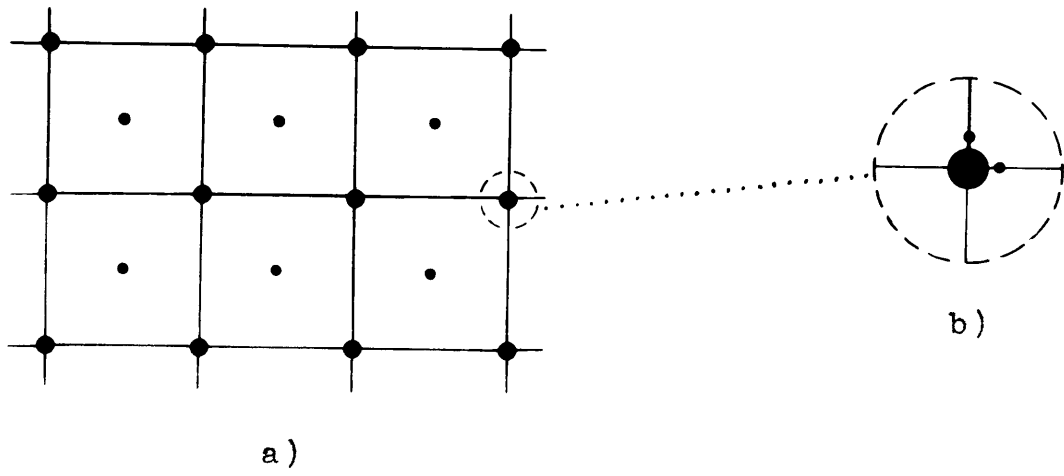
Fig. 2

(large circles), there were observed additional weak reflections (small circles) falling between the Nieuwenkamp-cell reflections. A possible supercell origin for these additional reflections can be discarded for the following reason. Their very low intensity would require a structure only slightly distorted from $P4_12_1$ symmetry, whereas the new diffraction symbol (obtained when the additional reflections are treated as superstructure reflections) would require drastic deviation from this symmetry.

Although not observable on the precession photographs, further examination of the crystals on a counter diffractometer showed additional weak reflections satellitic to some of the Nieuwenkamp-cell reflections, as shown exaggerated in Fig. 2B. The location and number of the satellitic reflections as well as the extra reflections mentioned above can be accounted for by twinning. The twin operations may be choosen as 90° rotations about the [110] and [$\bar{1}$10] directions of the primitive tetragonal cell (see Fig. 1A). These two operations relate a reference twin individual with two other twin individuals, the three comprising the composite twin as shown in Fig. 1B.

On the basis of the relationship between the twin individuals the indices of the additional reflections may be tentatively assigned. The intensity of a reflection from one individual may then be plotted against the

intensity of the same reflection from a second individual
for all the single, non-superposed reflections which are
individually measureable. The linearity of such plot con-
firms the indexing of the additional reflections and thus
confirms the relationship between the twin individuals.
Figure 3 shows such plots made with the crystal used for
intensity measurements. The precision of measurement of
the additional reflections is low due to their weak in-
tensities. Taking this into consideration, the plots are
satisfactorily linear.

Collection of intensity data

A small pseudooctahedron, 0.15 mm on a side, was
selected for intensity measurements. An equi-inclination
diffractometer employing a proportional counter was used
to collect integrated intensities with nickel-filtered
CuK radiation. The λ /2 harmonic was removed by pulse-
height analysis.

The single, nonsuperposed reflections presented no
problem in their measurement. On the other hand, the
composite, superposed reflections are somewhat spread
out as can be seen from Fig. 2B. To ensure collection
of the entire composite intensity an extended ω scan, as
well as a large counter aperture, was used.

About 200 reflections, including a number of the
same reflections from the different twin individuals,

Figure 3. Graphs of the integrated intensity of non-Superposed reflections from one twin individual plotted against the integrated intensity of the same nonsuperposed reflections from a second twin individual. I, I' and I'' represent the integrated intensity of reflections from the first, second, and third twin individuals, respectively.
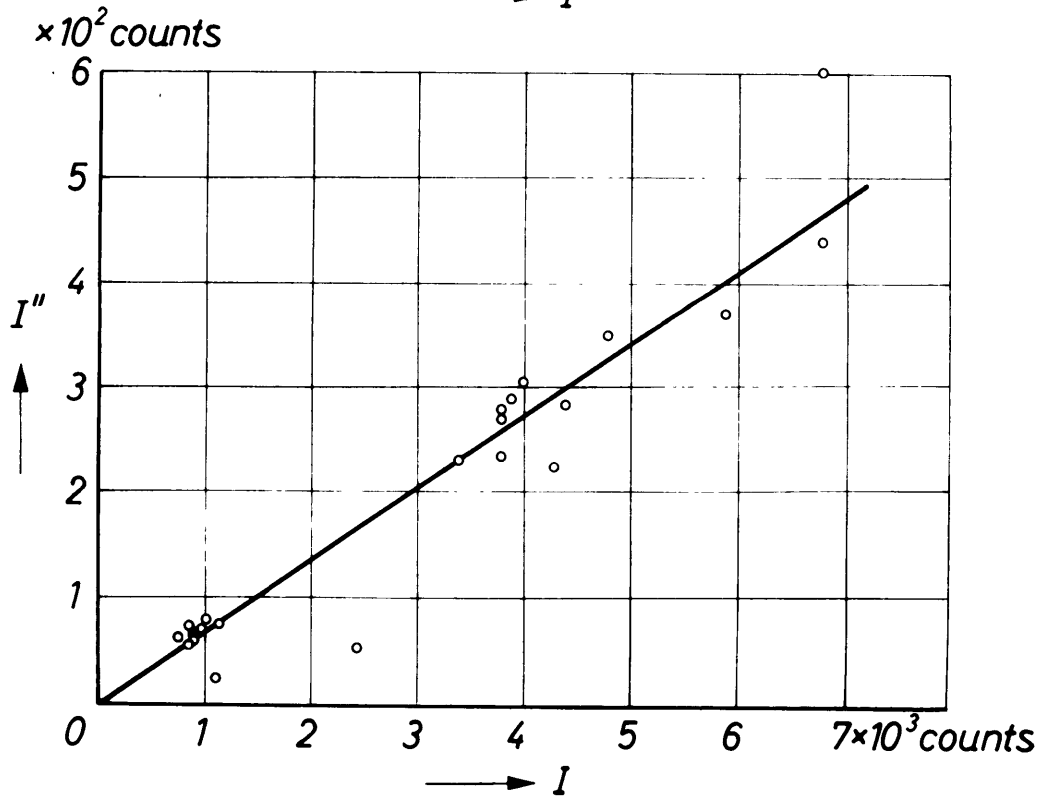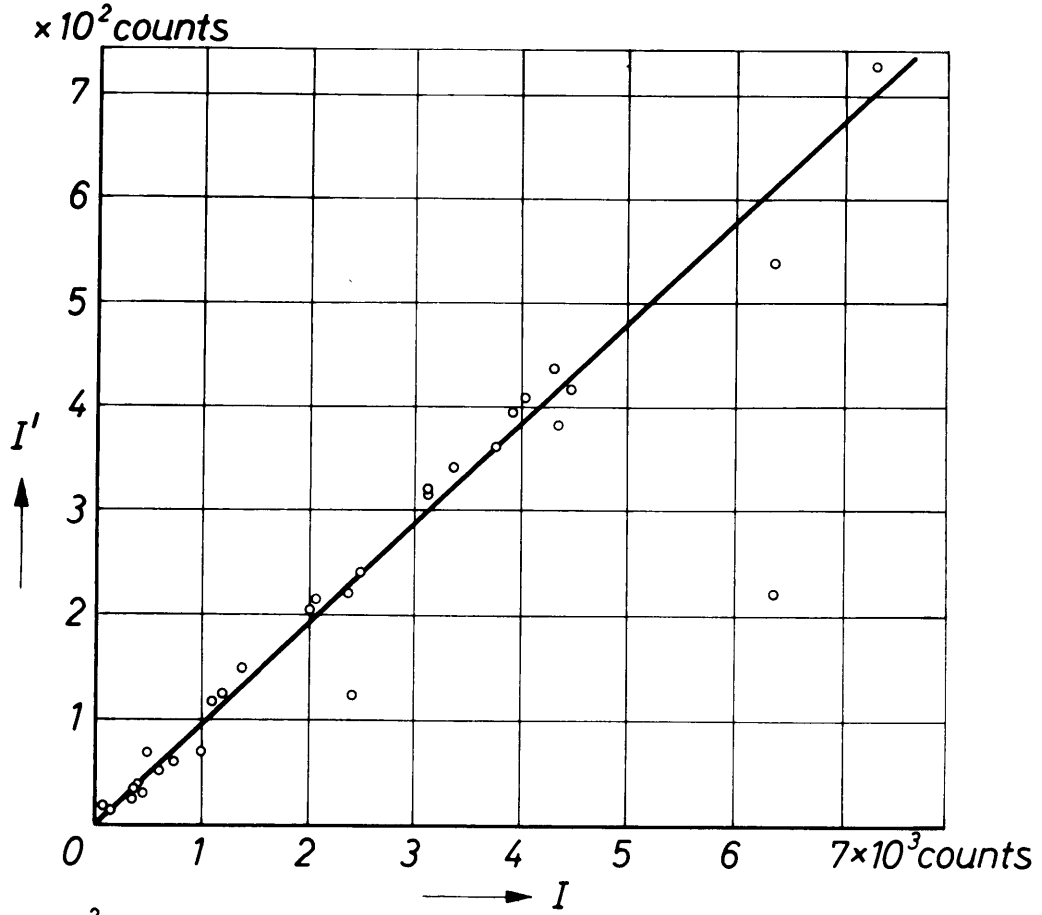
were collected. The data were corrected in the usual way. Since $\mu r=0.6$, no absorption correction was applied.

Correction of the data for twinning

It is possible to extract a set of individual intensities from the composite reflections if the volumes of the twin individuals are not all equal. In order to obtain a sufficiently large and random set of intensities for least squares refinement it is desireable to use this extracted set of intensities as well as the intensities of the nonsuperposed reflections. Since the lattices of the twin individuals in the twinned position mismatch appreciably, it may be assumed that there is negligible coherence of the diffracted beam and that the intensity of the composite reflections is the sum of the intensities of the contributing individual reflections. Taking into consideration the volumes of the twin individuals, this relation between the composite and individual reflections is

$$C_{HKL} = t\,I_{hkl} + u I_{h'k'l'} + v I_{h''k''l''} \tag{1}$$

where t, u and v are the volumes of the twin individuals. Using the orientation of the largest individual of the twin as the reference orientation, the indices of the individual reflections are found by operating on the indices of the composite reflection with the matrices

25

$$\begin{pmatrix} 100 \\ 010 \\ 001 \end{pmatrix} \qquad \begin{pmatrix} \tfrac{1}{2}\tfrac{1}{2}\tfrac{1}{2} \\ \tfrac{1}{2}\tfrac{1}{2}\tfrac{1}{2} \\ 1\bar{1}0 \end{pmatrix} \qquad \begin{pmatrix} \tfrac{1}{2}\tfrac{1}{2}\tfrac{1}{2} \\ \tfrac{1}{2}\tfrac{1}{2}\tfrac{1}{2} \\ \bar{1}\bar{1}0 \end{pmatrix}$$

These are respectively the unit matrix and the matrices representing the twin operations given above. In practice, the volumes $\underline{t}$, $\underline{u}$ and $\underline{v}$ are difficult to determine directly, so the volume ratios, $1=t/t$, $\mu=u/t$, and $\nu=v/t$, are used. These may be accurately estimated from the intensity ratios of the nonsuperposed reflections plotted in Fig. 3. The upper plot gives $\mu = 0.094$ and the lower plot gives $\nu = 0.064$.

Although the individual intensities may be obtained by the normal methods of solving a set of simultaneous equations, for computer solution an iterative method is advantageous and was employed. The recursive formula used was

$$^{i+1}\underline{I}_{hkl} = \underline{C}_{HKL} -\mu\,{}^{i}\underline{I}'_{h'k'l'} -\nu\,{}^{i}\underline{I}''_{h''k''l''} \qquad (2)$$

where the left superscript refers to the $\underline{i}$th approximation of the term which bears the superscript. The starting approximation

$$^{1}\underline{I}_{hkl} = \underline{C}\,_{HKL} - \frac{\mu}{1+\mu+\nu}\underline{C}\,_{H'K'L'} - \frac{\nu}{1+\mu+\nu}\underline{C}_{H''K''L''} \qquad (3)$$

was employed. This method has the disadvantage that the convergence rate depends upon the ratios of the individual intensities, but in this case, due to the very small magnitude of μ and ν, uniform convergence was reached in five cycles.

Refinement

After correcting for the effects of twinning, a total
of 110 reflections with $F_0 > 0$ were available for least-
square refinement. The number of observations per vari-
able is greater than 15. The full-matrix least-squares
refinement program written by C. T. Prewitt was used.
Scattering curves for both neutral and half-ionized atoms
were tried without any significant change in the results.
An equal-weighting scheme was employed. The original atom
coordinates of Nieuwenkamp, together with the best fit of
scale factor and isotropic temperature factors, yielded
an R value of 13%. Six cycles of refinement varying all
parameters led to convergence and a final R value of 4.4%.
The final observed and calculated structure amplitudes
are given in Table 1. During the refinement the silicon
atom oscillated to both sides of the Nieuwenkamp value
but finally settled within one standard deviation of his
value.

The final atomic parameters are given in Table 2
along with those of Nieuwenkamp. The silicon atom occupies
the position with site symmetry 2 in space group $P4_1 2_1$
while the oxygen atom lies in the general position. The
magnitudes of the temperature factors should not be re-
garded as very significant as the correlation factors
between these values and the scale factor are 0.82 and
0.64. The usual interaction of these dependent variables
is further aggravated in this case by the small number

Table 1

Comparison of observed and calculated structure amplitudes

h k l	F_o	F_c	h k l	F_o	F_c
0 0 4	10181	10643	0 4 1	9526	9502
8	3267	3458	2	5080	5156
0 1 1	20798	21729	3	6384	6345
2	10861	10852	4	3055	2684
3	1703	1524	5	4836	4902
4	4394	4311	6	1477	1574
5	10757	10979	0 5 1	1785	2480
6	1253	476	2	7005	7270
7	4633	5026	4	2882	2698
0 2 0	18967	19755	1 1 0	2928	2936
1	1817	1262	1	8738	8700
2	8026	7797	2	8222	7466
3	9804	9516	3	11738	11603
4	9245	8964	4	957	1092
5	3447	3561	5	1332	1488
6	1649	1614	6	12415	12331
7	4777	4731	1 2 0	828	358
8	3503	4201	1	5259	5131
0 3 1	12699	12718	2	8896	8630
2	12130	11958	3	5494	5050
3	6658	6030	4	8734	8512
4	618	642	5	7923	7909
5	1108	1424	6	1469	1122
6	5229	5412	7	5500	5753
0 4 0	3021	3820	1 3 0	4219	4231

h k l	F_o	F_c	h k l	F_o	F_c
1 3 1	7938	7732	2 2 7	5774	5534
2	8384	7835	2 3 1	6084	5674
3	8990	9923	2	9296	8879
4	6114	5851	3	7769	7495
5	4310	4068	4	3919	4097
6	3592	3760	5	3384	3419
7	3052	3438	6	4520	4417
1 4 0	11291	11032	2 4 1	7110	7006
1	3438	3318	2	5250	5120
2	3014	3083	3	4722	4504
3	2689	2533	4	2079	2755
4	8217	7981	5	4232	4347
5	2930	3215	2 5 0	1629	2208
1 5 0	2973	3147	1	2707	2790
1	4517	4419	2	4959	4911
2	479	969	3	2911	2633
3	3505	3750	4	1988	1662
4	2491	2493	3 3 0	7362	7316
2 2 0	5910	5387	1	6487	6307
1	1897	1838	2	7156	7117
2	3883	3565	3	5303	5287
3	9394	8971	4	5485	5503
4	7885	7590	5	2567	22526
5	4120	4297	3 3 6	798	779
6	3564	3513	3 4 0	6956	6932

h k l	F	F
3 4 1	5066	5051
2	2606	2451
3	5563	5860
4	3745	3842
3 5 0	5945	5610
1	2890	2846
2	1001	1245
4 4 0	2478	2946
1	3118	3394
2	6205	6773

Table 2

Final atomic parameters#

	x	σ_x	y	σ_y	z	σ_z	B
S1	.30004	.00033	-	-	-	-	0.83 A^2
S1$_N$	.300	.005	-	-	-	-	-
O	.23976	.00089	.10324	.00085	.17844	.00052	1.55
O$_N$	.245	.005	.100	.010	.175	.005	-

#The subscript, N, refers to Nieuwenkamp's original
values

of temperature factors and the rather narrow range of $(\sin\theta)/\lambda$ values. The correlation factor between the two temperature factors is smaller, implying that the ratio of the temperature factors is more meaningful than their individual magnitudes. The value of this ratio for low cristobalite is similar to those observed in other silicate refinements.

There are two independent silicon-oxygen distances and four independent oxygen-silicon-oxygen angles in the tetrahedron. The refined coordinates yield the values given in Table 3. The silicon-oxygen-silicon angle between joined tetrahedra is also included. The difference between the Si-O distances is not statistically significant. The deviations of the angles from the ideal tetrahedral angle are as much as three standard deviations and may be significant.

Table 3

Interatomic distances and angles

$Si - O_1$	$1.601 \pm .004$ A
$Si - O_2$	$1.608 \pm .004$
$O_1 - Si-O$	$111.5 \pm .3°$
$O_3 - Si-O_4$	$109.2 \pm .3$
$O_1 - Si-O_3$	$108.2 \pm .3$
$O_1 -Si-O_4$	$109.9 \pm .3$
$Si-O-Si$	$146.8 \pm .3$

Tom F. W. Barth (1932a), The cristobalite structures: I. High-cristobalite. Amer. Jour. Sci. 23, 350-356.

Tom F. W. Barth (1932b), The cristobalite structures: II. Low-cristobalite. Amer. Jour. Sci. 24, 97-110.

Clifford Frondel (1962), The system of mineralogy, 7th ed., vol. III, Silica minerals, John Wiley and Sons, New York, New York.

W. Nieuwenkamp (1935), Die Kristallstruktur des Tief-Cristobalts SiO_2. Z. Kristallogr. 92, 82-88.

W. Nieuwenkamp (1937), Uber die Struktur von Hoch-Cristobalit. S. Kristallogr. 96, 454-458.

A. van Valkenburg Jr. and B. F. Buie (1945), Octahedral cristobalite with quartz paramorphs from Ellora Caves, Hyderabad State, India. Amer. Min. 30, 526-535.

R. W. G. Wyckoff (125), The crystal structure of the high temperature form of cristobalite (SiO_2). Amer. Jour. Sci. 9, 448-459.

Chapter III

Symmetry and twinning of tridymite from the Steinbach,
Crab Orchard, and Esterville meteorites.

Abstract

Single-crystal x-ray examination of tridymites from
those meteorites mentioned in the title and of an arti-
ficial tridymite from silica brick, show them all to be
identical. At room temperature the symmetry is monoclinic,
Cc or C2/c with a = 18.54, b = 4.99, c 23.83 $\overset{\circ}{A}$, and
β = 105.65°. The cell contains 48 SiO_2 formula units.
The [20$\bar{1}$] direction of this cell is a pseudohexagonal
axis and all crystals examined were multiply twinned with
this axis as the six-fold twin axis. The pseudohexagonal
composite cell has dimensions; A = 30.0 and C = 49.3 $\overset{\circ}{A}$.

Tridymite is an accepted and not infrequent consti-
utent of meteorites.[1,2] With the exception of a set of
cell dimensions proposed for one meteoritic tridymite[3],
no crystallographic data have been reported which would
allow comparison of meteoritic tridymites with each other
or with artifical and natural, terrestrial occurrences of
tridymite. As a part of a crystallographic study of the
phases of silica, this note reports such new data for the
two mesosiderites: Esterville and Crab Orchard and the
siderophyre: Steinbach.

Identification as tridymite

Tridymite specimens from the three meteorites were
kindly made available from the Harvard Museum collection
by Professor Clifford Frondel. A thorough characteriza-
tion of these tridymites, including refractive indices,
specific gravity and x-ray powder patterns, as well as a
complete wet chemical analysis of the Steinbach tridy-
mite (J. Ito, analyst) is reported by Dr. Raymond Grant.[4]

As part of this study it was confirmed that the
Steinbach material is tridymite on the basis of its re-
versible transformation to high tridymite whose crystal
structure was determined on the same material. In addition
a spectrographic analysis, kindly run by Professor
Wm. H. Dennen, confirmed the unusually low impurity con-
tent of this tridymite. (See Table 1.)

Table 1

Spectrographic analysis of impurities in tridymite
from Steinbach meteorite (analyst: Wm. H. Dennen).

Al	400 ± 50	ppm
Na	270 ± 50	"
Mg	tr	
Fe	tr	
K	50	"
Li	10	"

Determination of the apparent cell

Using single-crystal methods some two dozen crystals from the three samples were studied. In all cases the apparent cell found was pseudohexagonal with the same dimensions reported for the Grimma meteorite tridymite[3] (part of the same fall as Steinbach). A very similar cell has been reported for tridymite from a gas-retort silica brick[5], "which had been heated for about 1900 working days at an average temperature of 1380° C".

To substantiate the apparent equality of the meteoritic and silica-brick results, a similar study was made of a silica-brick tridymite kindly provided by Dr. Helmut Stützel of Heinrich Koppers G.M.B.H. This tridymite has a somewhat similar history to that described above, being from a tunnel oven brick that had been heated for many years at 1400° C. The apparent cell of this material was found to be identical to that shown by the meteoritic tridymites. These cells are compared in Table 2.

Twinning

This apparent cell is, however, the twin-composite cell, twinning being suggested by the observations:

1) That all grains, including the (few) cases where twinning was optically readily apparent, showed the same 30 x 49 Å cell (hereafter called the composite cell).

Table 2

Comparison of apparent room-temperature cells

of tridymite from various sources.

This study	Grimm	Gas-retort silica brick
$A = 30.056$ Å	30.05 Å	30.08 Å
$C = 49.32_7$	49.56	49.08
pseudohexagonal	(cell given as orthohexagonal)	"appeared to be hexagonal"

2) That the composite cell shows systematic extinc-
tions which do not correspond to any possible
symmetry element (so called "non-crystallographic
extenctions"). Of each 54 composite reciprocal-
lattice nodes, only seven are present and 47 are
systematically extinct. The present reflections
are given by the conditions H and/or $K = 6\underline{n}$
and $H + K + L$ and/or $H + K - L = 6\underline{n}$. (Following
convention, capital letters refer to the compos-
ite cell.)

3) That although there is strong hexagonal pseudo-
symmetry and, within the limit of measurement,
exact hexagonal dimensionality, the composite
intensities show no true symmetry at all, except
for the center added by Friedel's law.

4) That the intensity ratios of pairs of reflections
vary from grain to grain.

A typical precession photograph taken in one of the
$\underline{A}$-axis directions is shown in Figure 1. The obvious twin-
ning seen in this direction may be described by a two-fold
rotation about the $\underline{C}$ axis. Examination of the other two
$\underline{A}$-axis directions showed the same twinned pattern but with
uniformly subdued or enhanced intensities implying similar
twinning in these directions, and thus a total of six twin
individuals in all. The two individuals seen in any $\underline{A}$-axis
photo are related to the pair seen in any other $\underline{A}$-axis
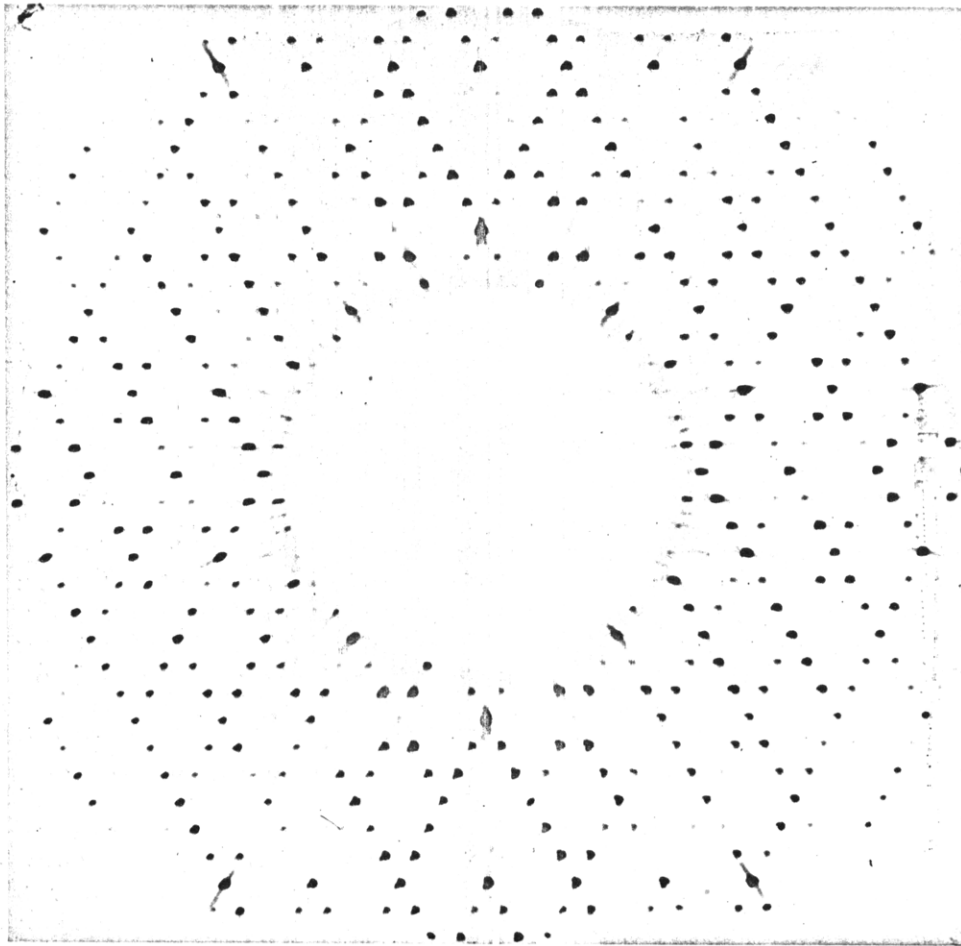photo by the operation of a three-fold twin axis parallel

Fig. 1. Sixth-level, A-axis precession photograph (referred
to composite cell) of Steinbach tridymite, taken with fil-
tered copper radiation. The C axis of the composite cell
is horizontal.

to $\underline{C}$. The six individuals of the twin can be equivalently related by the operations of a six-fold (twin) axis parallel to the pseudohexagonal axis of the composite cell.

Proposed true cell

From a knowledge of the twin operations, the collection of reflections due to one twin individual may be extracted from the composite. Figures 2 and 3 are projections along the twin axis of the reflections present in the composite cell and in one of the twin individuals, respectively. Figure 4 shows the reflections of one twin individual plotted in the direction of the composite $\underline{A}$ axis (as seen in Figure 1). The zero, first, and second reciprocal-lattice levels normal to this direction are shown, as well as the superposition of all three levels. This collection of reflections shows diffraction symmetry $2/\underline{m}$ $\underline{C}$ -/$\underline{c}$ and no non-crystallographic absences. The space group is therefore $\underline{C}$ $2/\underline{c}$ or $\underline{Cc}$ depending on the presence or absence of a symmetry center, respectively. The reduced monoclinic cell has dimensions $\underline{a} = 18.53_5$ Å, $\underline{b} = 4.99_3$ Å, $\underline{c} = 23.83_2$ Å, $\beta = 105.65°$. The cell volume is 2124 Å^3 which yields a cell content of 48 SiO_2 formula units when the published[2] value of 2.26 is used for the density.

The unique monoclinic axis $\underline{b}$ coincides with the $\underline{A}$ axis of the composite cell. The relations of the other axes to those of the composite cell axes can be seen in

Fig. 2.   Pattern of all observed
x-ray spectra referred to the
composite reciprocal lattice.
The numbers refer to the $\_$
indices mod 6.

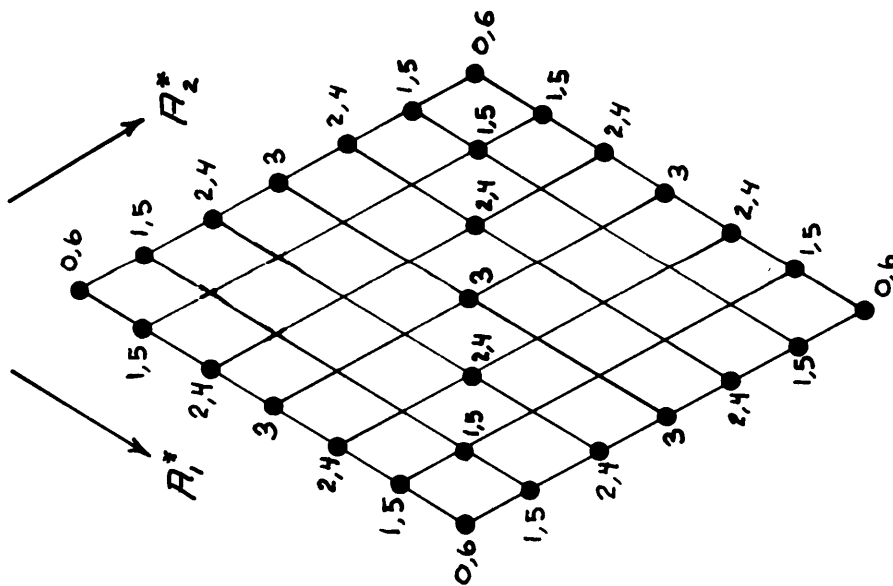Fig. 3.   Pattern of
x-ray spectra due
to one twin individ-
ual.
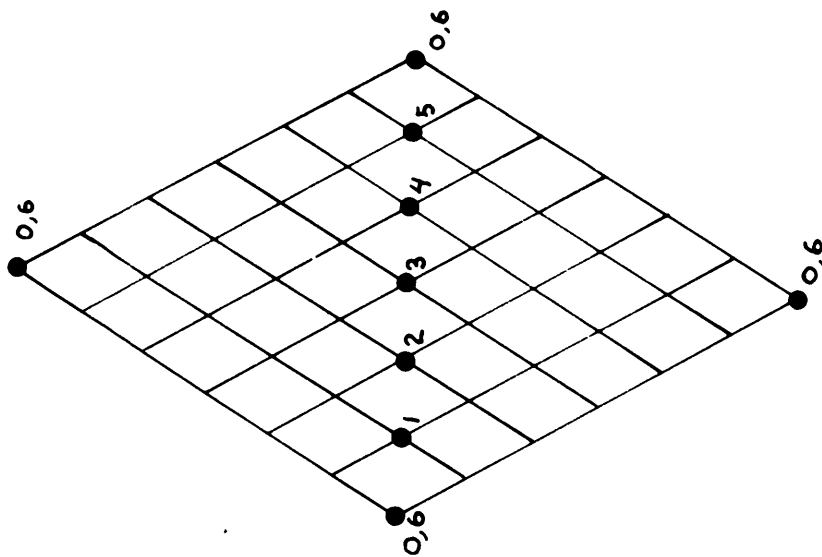
Fig. 4. Reciprocal-lattice levels normal to the $\underline{A}$ axis of the composite cell, showing pattern of reflections due to one twin individual. Capitals labels refer to composite cell, lower-case labels to true (untwinned) cell.

C*

A*

Zero level

1st level

a*

c*

0, 1 and 2 levels

2nd level

45
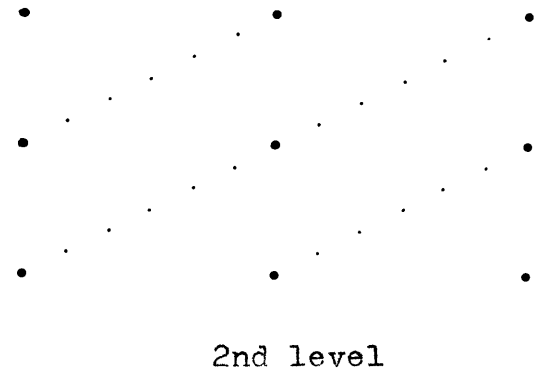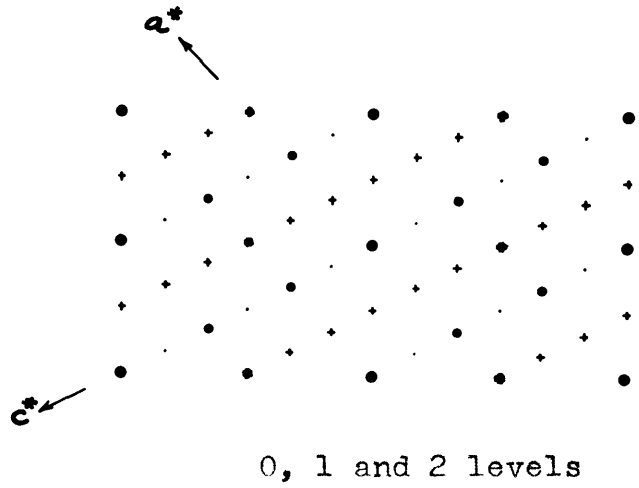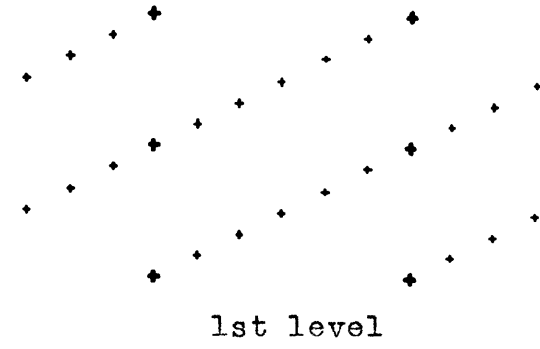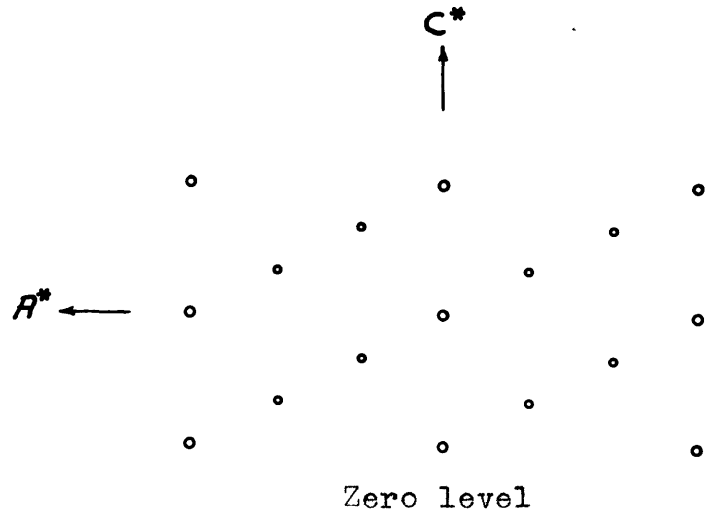
Figure 4. The matrix, T, relating the true cell with the composite cell is 1, $\bar{1}$, 2/3,3,1/1,$\bar{1}$,$\bar{1}$, i.e. A = aT.

Check of monoclinic symmetry

A set of diffraction intensities from a twinned grain was collected with a single-crystal diffractometer out to a value of sin Θ/λ = .5 for purposes of a crystal structure determination which is in progress. Due to the twinning some, but not all of the reflections are identically superposed. For the general case, assuming no coherence in the diffracted beams from different twin individuals, the $\underline{h}$'th composite measured intensity is given by

$$C_h = \sum_{i=1}^{6} \nu_i \, I_{hT_i}$$

where $\underline{T_i}$ is the $\underline{i}$'th twin operation matrix, ν_i is the volume of the twin individual related to a reference individual by the operation T_i and I is the true intensity. Then the $\underline{j}$'th member of the twin-equivalent set of compsite intensities is given by

$$C_{hT_j} = \sum_{i=1}^{6} \nu_i \, I_{hT_jT_i}$$

This set of equations can then be solved for the true intensities according to the matrix equation

$$I_h = \nu_{hk}^{-1} \, C_k$$

if the volumes of the twin individuals are not all equal. The volumes (relative to one individual taken as unit volume) are easily determined by measurement of equivalent, non-superposed reflections from each of the individuals.

As noted above, the composite cell has Friedel symmetry $\bar{1}$, whereas the true cell has Friedel symmetry 2/$\underline{m}$. Thus half of the extracted true intensities must equal the other half by the additional symmetry element of the true cell. In general, the agreement between such pairs is a function of the seventeen variables of the last equation. The average agreement, $\sum |I-I'| / \sum (I+I')$, for all of the intensities collected that were affected by twinning was 0.032, which strongly substantiates the previous conclusions in regard to the cell and symmetry.

Relation to the high tridymite structure

At about 107° C this tridymite transforms rapidly and reversibly to another polymorph whose structure was found to be only a slightly distorted version of the ideal high-tridymite structure[6]. Thus, it can be expected that the room-temperature form will also be similar in structure to high tridymite. When the atom locations of the high-tridymite cell are transformed to their corresponding locations in the room-temperature cell, it can be seen that, if the symmetry is cetrosymmetric ($\underline{C}$2/$\underline{c}$), there are six SiO_2 formula units per asymmetric unit; in this case three oxygen atoms are constrained to inversion centers. This, of course, constrains their Si-O-Si bonds to be 180°. If the symmetry in acentric ($\underline{Cc}$), there are twelve formula units per asymmetric unit, with all atoms in the general position.

Summary

Tridymite from three meteorites and a silica brick were found to be identical and to show the same apparent cell as had previously been reported separately for a meteoritic tridymite and a silica brick tridymite. Twinning, however, seems to be universally present and the apparent cell is actually the twin composite cell. The twin is composed of six individuals related by the operations of a six-fold twin axis. The true symmetry is monoclinic with a cell volume twelve times that of the classical high tridymite cell.

Brian Mason, 1962, Meteorites, J. Wiley and Sons, New
     York, New York.

Clifford Frondel, 1962, Dana's, The System of Mineralogy,
     vol. III, Silica minerals, J. Wiley and Sons, New
     York, New York.

Wolfgang Götz, 1962, Untersuchungen am Tridymit des
     Siderophys von Grimma in Sachsen, Chem. d. Erd., 22,
     167-174.

Raymond Grant, 1965, Ph. D. Thesis, Harvard University.

J. E. Fleming & F. Lynton, 1960, A preliminary study of
     the crystal structure of low tridymite, Phys. Chem.
     of Glasses, 1, 148-154.

Wayne A. Dollase, 1966, Ph. D. Thesis, M. I. T.

Chapter IV

A dynamic superstructure associated
with the high-low transformation in tridymite

Abstract

A weak superstructure has been observed in a 70° C range directly above the low-to-high transformation in tridymite. The supercell reflections lie in, or very nearly in one of the [[110]] directions of the high-tridymite (pseudo)hexagonal subcell. The intensities of the supercell reflections fall off very rapidly away from the subcell reflections, giving the appearance of satellites. As the temperature is increased, the "satellites" move away from their respective subcell reflections and decrease in intensity. Over the 70° C range in which they are visible, the variable satellite spacing represents, in real space, an apparently continuous decrease in supercell period from about 105 Å down to about 65 Å.

The high-low (beta-alpha) transformation in tridymite
has the characteristic of a distortional transformation,
(Buerger, 1961). This low-energy, non-quenchable phase
transformation takes place rapidly and reversibly within
a small temperature range at slightly above 100° C. As
a part of a structural study of the phases of silica, this
transformation was studied by single-crystal x-ray diffrac-
tion methods. This paper reports observations made of an
unusual superstructure which appears to be associated with
the distortional transformation, and which is characterized
by a supercell translation that varies remarkably with
temperature.

Film observations

The high-low transformation of a tridymite crystal
from the Steinbach meteorite was monitored with Laue
photographs taken at small temperature intervals from
room temperature to 250° C. The transformation is marked
by the sudden disappearance of the reflections character-
izing the low-temperature supercell. Along with the dis-
appearance of these reflections, many of the remaining
"subcell" reflections develop a series of very weak satel-
litic maxima, whose intensities decline rapidly away from
the strong subcell reflection, somewhat similar in aspect
to the secondary maxima of optical diffraction described
by the $(\sin x/x)^2$ function.

As the temperature is increased the satellites are
observed to decrease in intensity and to increase their
separation from their respective main peaks. These changes
appear to occur continuously from the transformation point
at about 107° C up to about 170° C. At this point the
satellites have decreased in intensity until they are no
longer discernable above the background. The regularity of
the directions and spacings of the satellitic reflections
indicates that they form a periodic superstructurew whose
cell changes greatly in size with temperature.

This behavior was entirely reversible with temperature
(although the transformation itself shows hysterisis), and
could be repeated at will on other crystals of the same tridy-
mite sample. Similar studies were made with tridymite crys-
tals from several terrestrial, volcanic occurrences which
are characterized by different low-temperature supercells.
Except that their low-to-high transformations occurred at
a higher temperature (about 125° C) the appearance of satel-
lites and their behavior with temperature was analogous with
the meteoritic tridymite.

To obtain the orientation of the supercell relative
to the normal high-tridymite cell, oscillation and precession
photographs were taken in this temperature range. The oscil-
lation photographs taken about the pseudohexagonal axis of
the high tridymite cell showed that the satellites were
restricted to the reciprocal lattice levels normal to this
axis. Iron-radiation precession photographs made of these

levels gave the pattern schematically reproduced in
Figure 1. An enlarged section of one of the actual photographs is shown in Figure 2.

The large spots of Figure 1 outline the normal high-tridymite reciprocal cell, whose axes have been designated by lower case labels. Referred to this cell the satellites can be seen to lie in (or approximately in) the direction of one of the a * axes. Thus in direct space the variable period repeat of the supercell occurs in one of the [[110]] directions of the high-tridymite cell. Measurements from precession photographs taken in the temperature range of 110° to 170° C, gave supercell translations of about 65 to 95 Å.

The furnace employed in heating the crystal during the film observations was of the type described by Wuench (1963). With this type of furnace, and the use of long-wavelength radiation (necessary to resolve the closely spaced satellites) only a very limited range of diffraction angle, θ, was observable. In addition, the rather open nature of the furnace allowed the temperature to vary slightly and thus to change the diffraction effects during their observation. For these reasons an improved furnace was constructed (See appendix) based largely upon a design due to Buerger, et.al. (1943) This furnace was designed for use with an equi-inclination counter diffractometer so as to allow a range of upsilon up to 135°, and mu up to 45°, to be explored. In practice the furnace also provided the desired constancy of temperature,
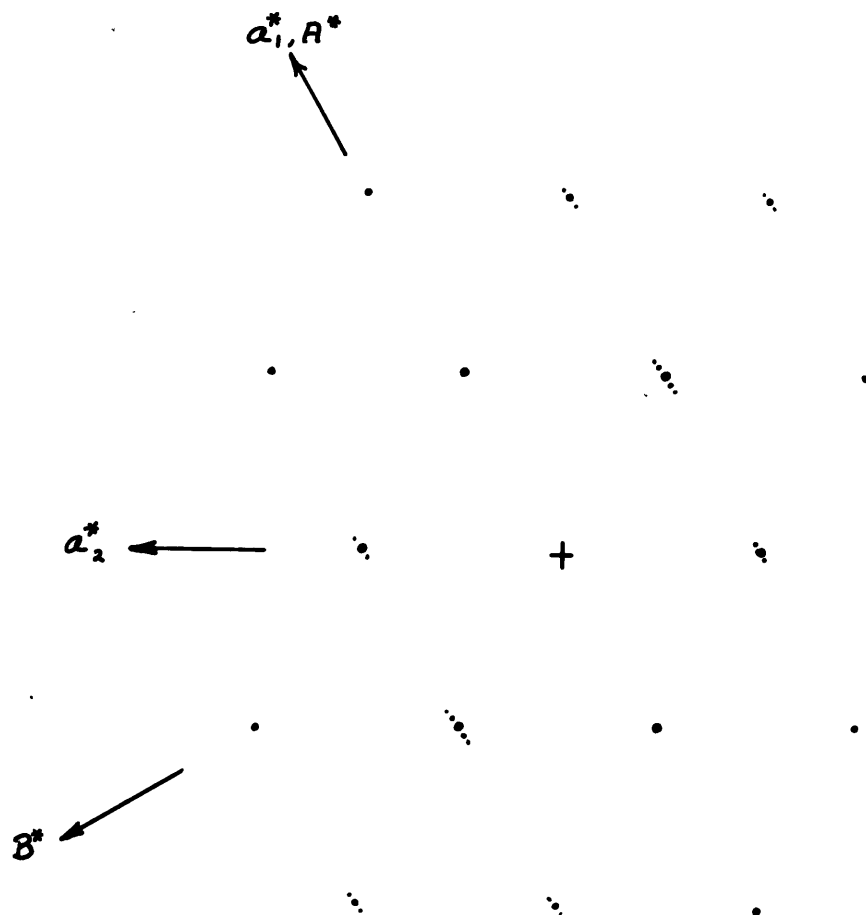
Figure 1. Schematic representation of a reciprocal lattice
level normal to the c axis, showing superstructure.
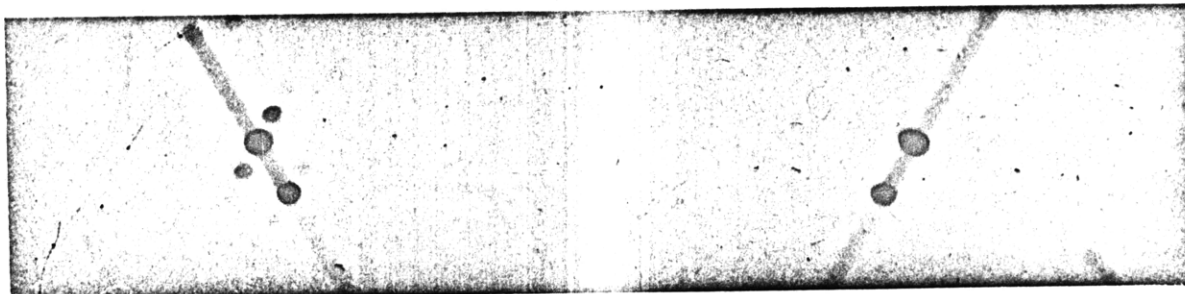
Figure 2. Enlarged section of an unfiltered, c-axis, zero-level precession photograph taken with iron radiation. The reflection showing satellites in 010, while that without satellites is 100. Beta reflections are also seen. 3X.

such that during the measurements at any given setting no
temperature variation effect could be noticed, after allow-
ing a short time for the furnace to come to equilibrium.

Single-crystal diffractometer observations

The diffraction effects observed with an equi-inclin-
ation counter diffractometer can be understood by refer-
ence to Figure 3 which shows an enlarged part of the stan-
dard nth level, equi-inclination geometry. (See for example,
Buerger, 1942, p. 255). The dashed lines represent three
successive positions of a single reciprocal-lattice line
passing through the sphere of reflection. The reciprocal-
lattice line, which lies in the plane of the figure, contains
a main reflection and two satellitic supercell reflections.
The three positions shown are those where successively, one
satellite, the main reflections, and the other satellite
are in the reflections position.

During such a scan the difference in the rotation
angle, $\Delta\phi$ between the reflecting positions of the satel-
lites on either side of the main peak, may be measured
directly from a strip chart recording. In principle, the
difference in the diffraction angle, $\Delta\tau$, between this
pair of satellites could also be measured directly, for
example, by means of a variable detector apperture. From
these two measurements it is possible to calculate the super-
structure parameters of direct interest, namely, the magni-
tude and direction of the superstructure translation. For
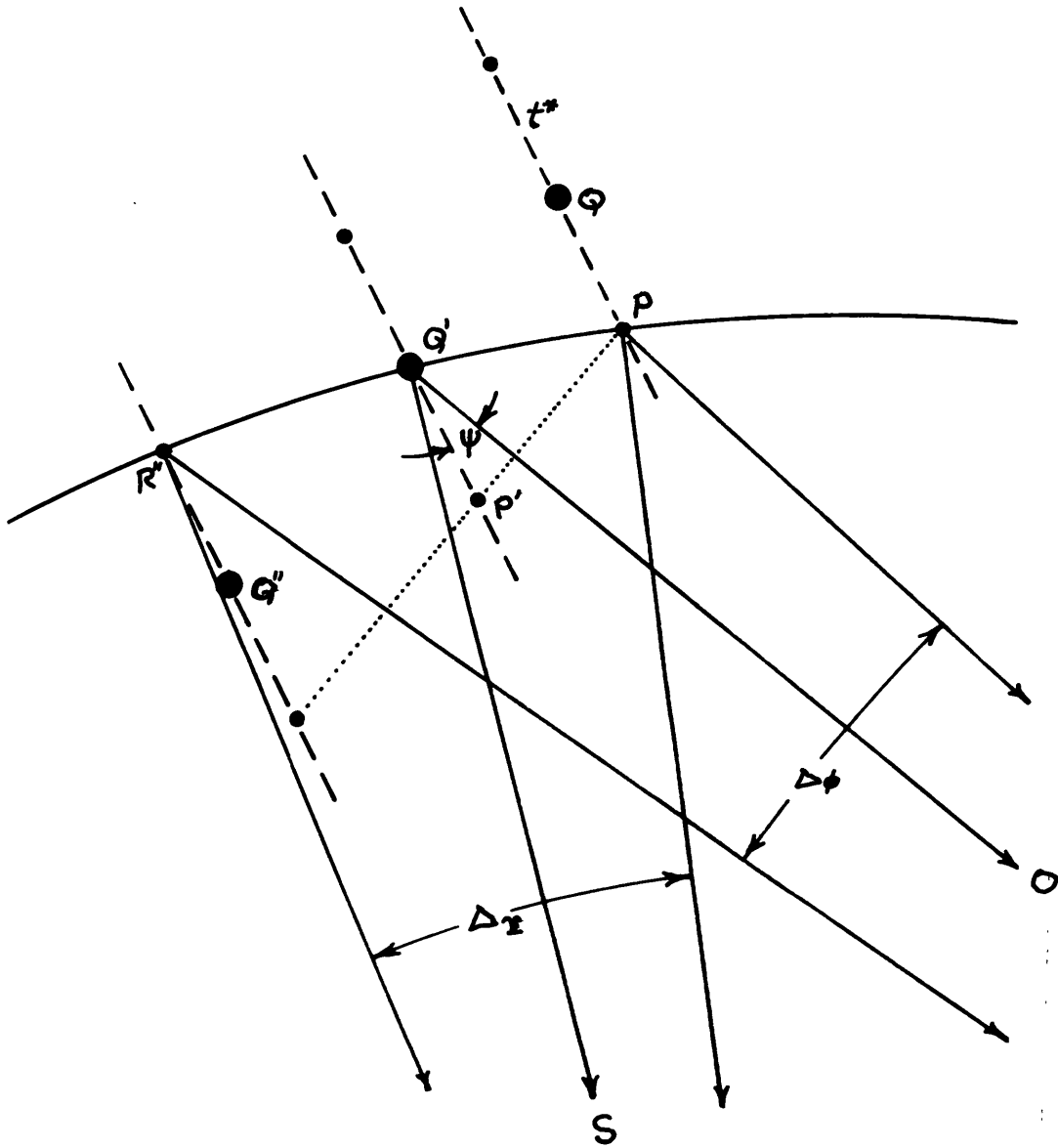
Figure 3.

this purpose it is convenient to specify the orientation
of the superstructure translation by the angle   it makes
with a radial to the main reflection, as shown in Figure 3.
An equation relating these variables may be derived from
Figure 3. Since the measurements on the weak satellites
cannot easily be made with high precision, it is sufficient
to derive an approximate equation.

If the superstructure period is very large, ie. if the
separation, t^{*}, of a satellite from its main reflection is
small, then:

$$\Delta \phi \approx \tan^{-1} \left(\frac{QQ''}{Q'O} \right)$$

(1)

where $QQ'' \approx 2(t^{*} \sin \psi + t^{*} \cos \psi \tan(OQ'P))$.

From equi-inclination geometry (Buerger, 1942, p. 255).

$$OQ'P = \Upsilon/2$$

$$Q'O = 2 \cos \nu \sin(\Upsilon/2).$$

Substituting these values in (1),

$$\Delta \phi \approx \tan^{-1} \left[\frac{2t^{*}(\sin \psi + \cos \psi \tan(\Upsilon/2)}{2 \cos \nu \sin(\Upsilon/2)} \right].$$

(2)

Multiplying the numerator and denominator of the arctan
argument by $\cos(\Upsilon/2)$ gives,

$$\Delta \phi \approx \tan^{-1} \left[\frac{2t^{*}(\cos(\Upsilon/2)\sin \psi + \cos(\Upsilon/2)\cos \psi \tan(\Upsilon/2)}{\cos(\Upsilon/2)2\cos \nu \sin(\Upsilon/2)} \right]$$

(3)

which can be simplified to

$$\Delta \phi \approx \tan^{-1} \left[\frac{2t^{*} \sin(\Upsilon/2) + \psi)}{\sin \Upsilon \cos \nu} \right].$$

(4)

Similarly,

$$\Delta \Upsilon \approx \tan^{-1} \left(\frac{PR''}{O'S} \right)$$

(5)

where

$$PR'' \approx 2 \cos \psi t^{*}/\cos(OQ'P).$$

Again from Buerger (1942),

$$\underline{OQ'P} = T/2$$

$$\underline{Q'S} = \cos \nu .$$

With these values substituted in (5),

$$\triangle_T = \tan^{-1} \left[\frac{2t^* \cos \psi}{\cos \nu \cos (T/2)} \right] . \tag{6}$$

In practice the parameter ψ was known from films and could be confirmed by scanning several equivalent reflections on the diffractometer. Equation (4) may then be solved for the superstructure translation which, converted to direct space, is:

$$t = \frac{\lambda}{t^*} = \frac{2\lambda \sin(T/2 + \psi)}{\tan \triangle_\phi \sin T \cos \nu} . \tag{7}$$

It can be noted from Figure 3 that, although (7) is based upon a number of approximations, they tend to be self-cancelling as long as the pair of satellites are considered rather than the difference in the rotation angle between a satellite and the main peak.

A large number of scans were made on the single-crystal counter diffractometer at temperatures between 20° and 250° C using several different crystals. A typical scan showing the satellites is reproduced in Figure 4. The main peak has been cut off due to the scaling necessary to show the satellite detail. The envelope shown in Figure 4 may be decomposed into its constituent main peak and satellites. The decomposed group is shown in Figure 5 with the main peak represented by the dashed line for clarity. As mentioned above, with an increase in temperature
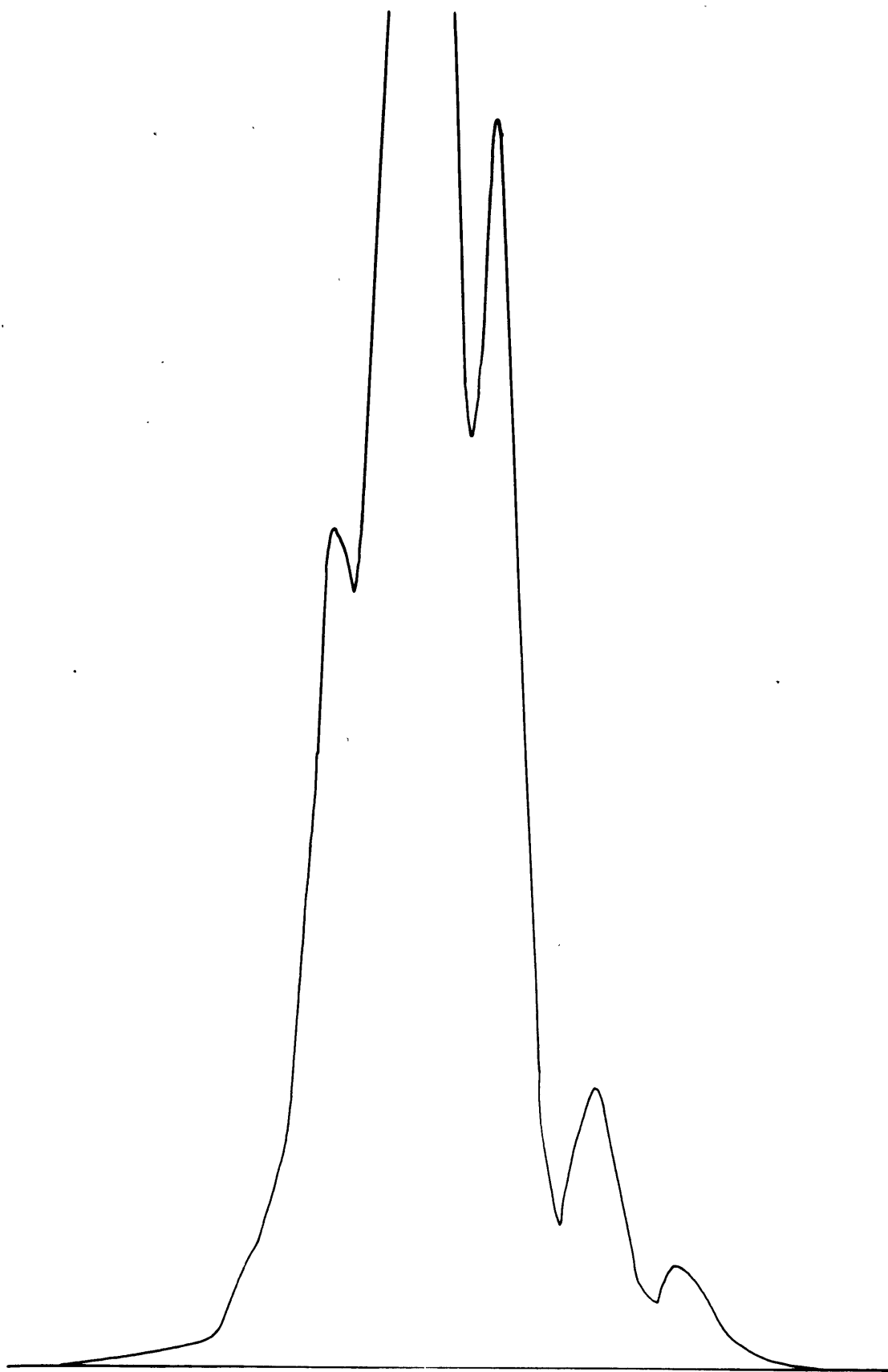
Figure 4. Diffractometer scan thru the 330 reflection of
the Steinbach tridymite, showing satellites.
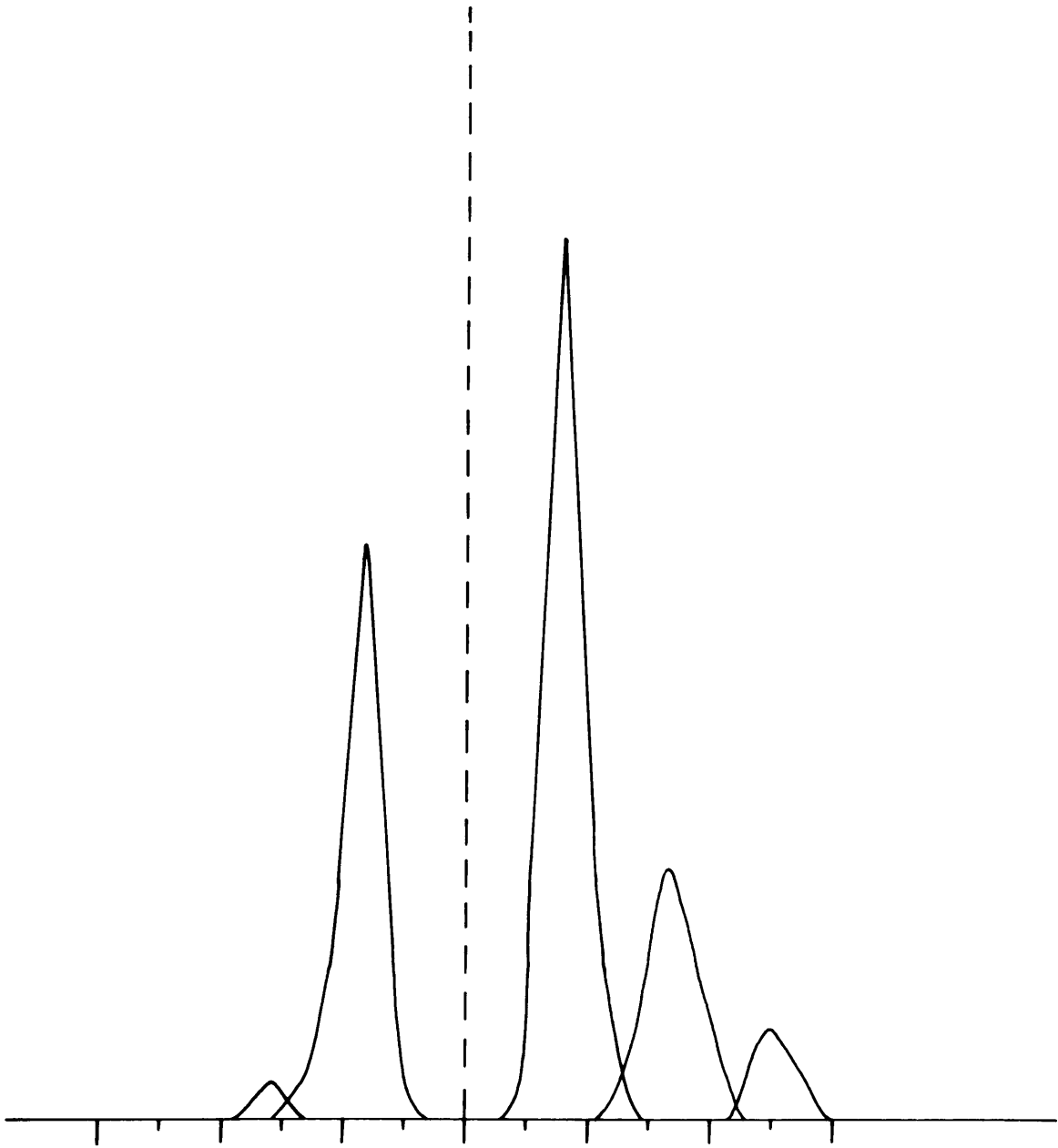
Figure 5. Decomposition of Figure 4 into its components.

the satellites spread away from the main peak and decrease in intensity. This effect is shown in Figure 6 by the superposition of two recordings made at two different temperatures. The greater value of Δ_ϕ for the higher-temperature recording (dashed lines) is obvious.

Using equation (7) the observed Δ_ϕ values were converted to the supercell translation, $\underline{A}$. The results for two reflections of the Steinbach tridymite are shown in Figure 7. The relationship between the temperature and the translation thus seems to inverse and linear. By slow reduction of the temperature it was found possible to undercool the transformation to the low form by about 15° C. The supercell translations found in the undercooled region seem to obey the same linear relationship. Furthermore, similar measurements made on several crystals of a terrestrial tridymite (from Plumas Co. California) showed that, although the transformation from the low form took place at a higher temperature (ca. 125° C), when the satellites did appear their spacing was also that given by the relation shown in Figure 7.

The low-form structures of the terrestrial and meteoritic tridymites are definitely different and, since they transform reversibly to themselves, their structures in the satellite range are probably also different. It seems therefore that the satellite spacing is independent of the actual transformation temperature and of the small differences in the structures of the tridymites.
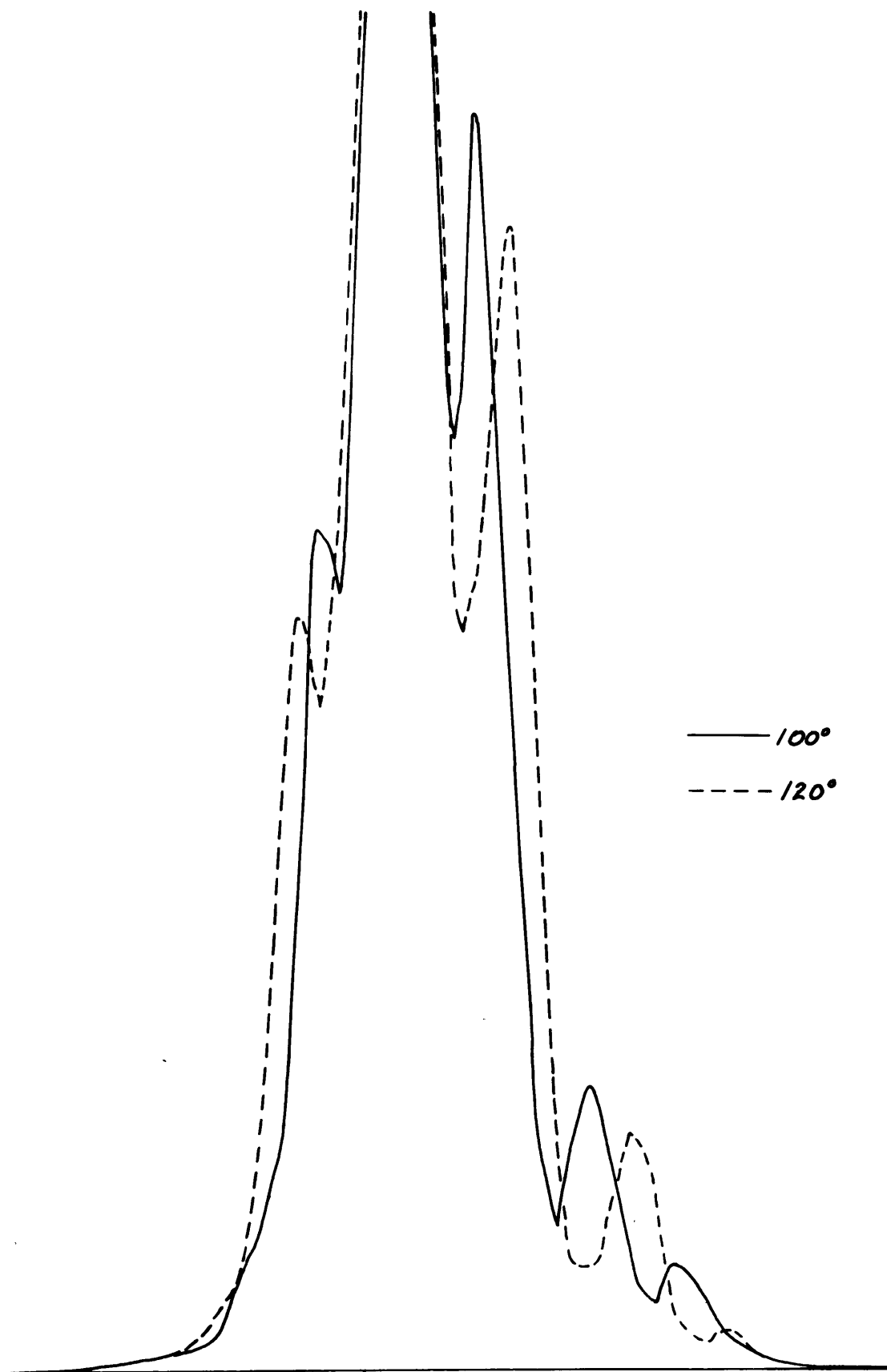
Figure 6. Superposition of the 330 scans at two different temperatures.
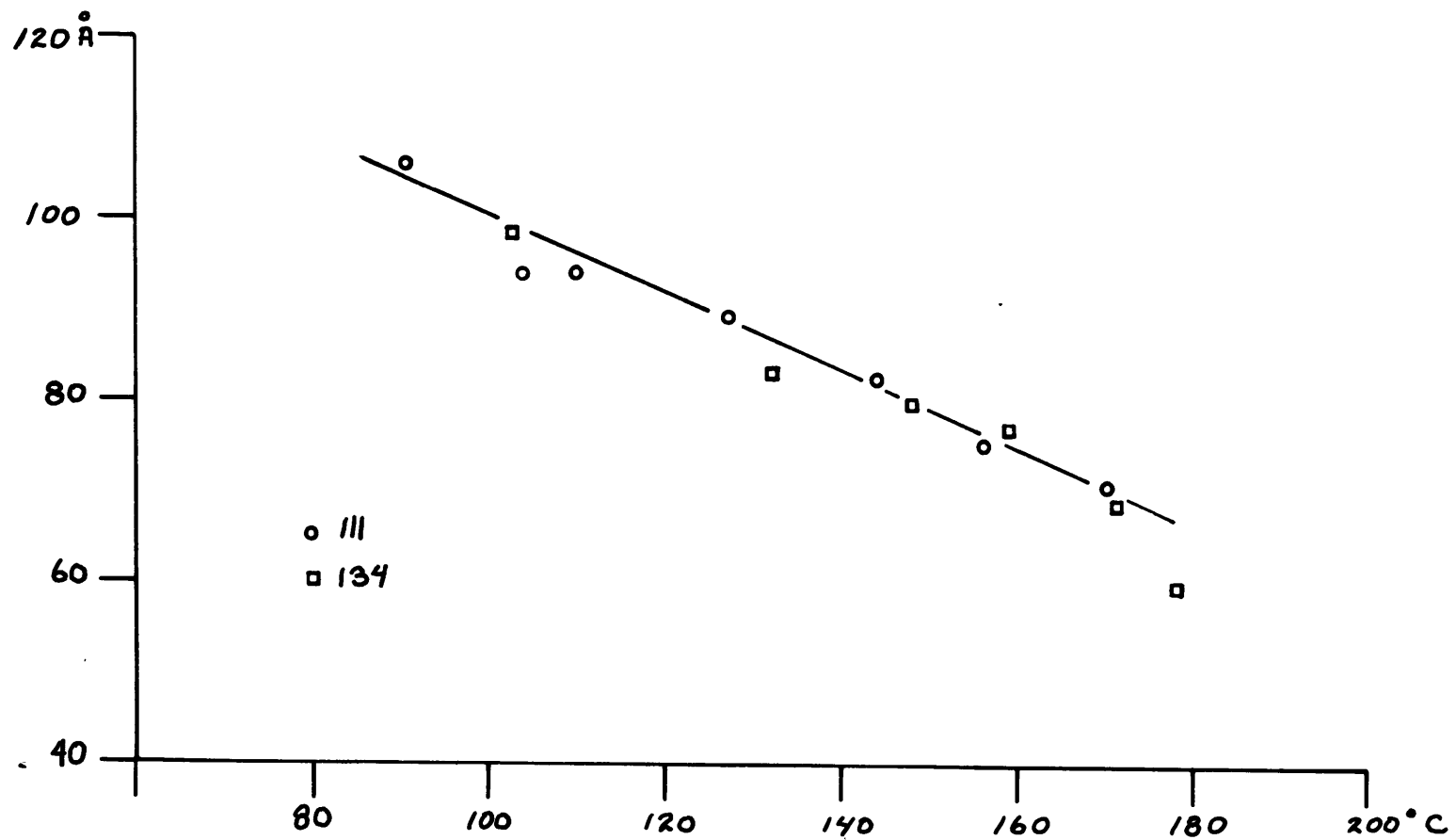
Figure 7. Relation between temperature and supercell period for two reflections of the Steinbach tridymite.

Previous observations and origin of the
superstructure.

Although the observations reported above were made
independently, it was pointed out to the author by
Dr. M. L. Canut-Amorós and Professor J. L. Amorós that
strikingly similar phenomena have been observed at the
ferroelectric transition in $NaNO_2$. Tanisaki (1961, 1963)
discovered that just above the Curie point the normal
x-ray reflections of $NaNO_2$ showed a pair of sharp satellites.
These satellites, which occur in the direction of the a
axis, are visible only over a 3° C range. Above this
temperature they become diffuse. The repeat period repre-
sented by the satellite spacing decreases from 9.4x a to
8.6x a as the temperature is increased over this 3° range.
These observations were confirmed by Canut and Mendiola
(1964).

An exact explanation of these effects in tridymite
(and $NaNO_2$), in terms of the changes in the atomic struc-
ture, will require a quantitative study of the satellite
intensities and their change with temperature. The pre-
sent information does, however, allow some speculative con-
clusions to be drawn.

It seems likely that the dynamic superstructure is
a result of correlation or interdependence between the
thermal vibrations of neighboring atoms (probably one or more
of the oxygen atoms in the case of tridymite). Such cor-
relation normally gives rise to thermal diffuse scattering,

that is, the correlations are non-periodic. See for example
the t. d. s. studies of Arnold (1965) on quartz where he
has quantitatively related the t. d. s. intensity with
correlated motion between chains of atoms.

At a distortional transformation the loose changing
structure evidently allows the correlations to become so
strong that the thermal displacements become more-or-less
ordered and periodic. Such superstructures may therefore
be generally found associated with distortional transfor-
mations.

Acknowledgements

Heinrich Arnold, 1965, Diffuse Rontgenbeugung und Kooperation
bei der α-β- Umwendlung von Querz, Zeit. Krist., 121,
pp. 145-157.

M. J. Buerger, 1961, Polymorphism and phase transformations,
Fort. Min. 39, pp. 9-24

M. J. Buerger, Newton W. Buerger, and Frank G. Chesley,
1943, Apparatus for making x-ray powder photgraphs
at controlled, elevated temperatures, Am. Min., 28,
pp. 285-302.

M. L. Canut and J. Mendiola, 1964, Critical scattering of
x-rays in $NaNO_2$, plys. stat. sol. 5, pp. 313-27.

Sigetosi Tanisaki, 1961, Microdomain structure in para-
electric phase of $NaNO_2$, J. Phys. Soc., Japan, 16,
pp. 574, only.

Sigetosi Tanisaki, 1963, X-ray study on the ferroelectric
phase tranition of $NaNO_2$, J. Phys. Soc., Japan, 18,
pp. 1181-19.

B. J. Wuensch, 1963, Ph. D. Thesis, M. I. T., also in
M. J. Buerger, 1964, The precession method, J. Wiley
and Sons, Inc., New York, New York, pp. 248-251.

Chapter V

The Crystal Structure at 220° C of high tridymite
from the Steinbach meteorite

Abstract

Tridymite from the Steinbach meteorite has been examined at 220° C and found to be orthorhombic, space group C222$_1$ with a = 8.74 Å, b = 5.04 Å, and c = 8.24 Å. The crystal-structure has been determined and refined using single-crystal counter-diffractometer data, to R = 8.6%. The resulting structure is distorted in comparison with the ideal high tridymite structure. The tetrahedra remain nearly regular but are twisted relative to each other. The magnitudes of the thermal displacements, especially of the oxygen atoms normal to their bonds with silicon atoms, are unusually large.

Tridymite from the Steinbach meteorite was found, from film and single-crystal diffractometer observations, to exist in three well defined structural states between room temperature and 250° C. Each of the phases is characterized by a different cell and symmetry. The highest-temperature polymorph of the three, existing from about 180° C up to the 250° limit of the investigated temperature range, is here termed high tridymite since it has the same small cell that has previously been reported for high tridymite[1]. This paper reports the results of a study of its crystal structure at 220° C. The details of the transformations and of the structures of the lower-temperature phases, as well as the relationship of the Steinbach tridymite to other tridymites, is considered elsewhere[2].

Previous structural studies of high tridymite

The first structural study of tridymite was that of high tridymite made by R. E. Gibbs in 1927. The source of the tridymite was not given. The unit-cell parameters were measured from Laue and oscillation photographs taken at an undetermined temperature "well above the transition point". Gibbs concluded that at this temperature the Laue symmetry was 6mmm, and that the reflections of the type $hh\cdot\ell$, $\ell = 2n + 1$ were absent. This symmetry and extinction rule restricted the possible space groups to a small number. The observed density and cell size require

the cell to contain four formula units of SiO_2. By further requiring the structure to be composed of regular SiO_4 tetrahedra, the space group could be limited to $\underline{P6_3/mmc}$. As noted by Gibbs, this fixed the structure as exxentially identical with that of ice.

The only other structural investigation made of tridymite above room temperature has been a powder-diffractometer study of a natural volcanic tridymite by Sato[3]. He reported that he observed a "good agreement" between 23 intensities measured on a powder diffractometer at 500° C, and the values calculated from the model proposed by Gibbs.

Symmetry of high tridymite

A specimen of tridymite from the Steinbach meteorite was kindly provided by Professor Clifford Frondel from the Harvard Museum collection. A previously reported study[2] has shown this material to be invariable twinned. The proportion of a grain in each of the possible twin orientations is easily measureable from the relative intensities of x-ray reflections not superposed by the twinning. By examining several dozen grains it was possible to select one with 3% of its volume in a twinned position relative to the main part of the grain. Precession and oscillation photographs were taken of this grain and of other less favorably twinned grains at temperatures in the range of 200° to 250° C, using a heating device similar to that described by Wuensch[4].

The photographs revealed strong hexagonal pseudosymmetry and a cell which is dimensionally hexagonal within the error of measurement. The true symmetry in this temperature range appeared to be orthorhombic as was latter verified from diffractometer measurements. The parameters of the $\underline{C}$-centered orthorhombic unit cell are given in Table 1. The only reflections found to be extinct were the odd orders of the $00\underline{\ell}$-type reflections. All other reflections were actually measureable on the diffractometer. The space group is therefore uniquely determined to be $\underline{C}222_1$.

The $\underline{C}$-centered cell has twice the volume of the ideal hexagonal cell and thus contains eight formula units of SiO_2. Since the multiplicity of the general position in space group $\underline{C}222_1$ is eight-fold, the asymmetric unit must contain one formula unit.

Data collection

Intensity measurements were made on a single-crystal counter-diffractometer employing equi-inclination geometry. The furnace used in heating the crystal was especially designed to hold the temperature constant over the data-collection period and to allow the maximum possible volume of reciprocal space to be explored. In this design the primary and diffracted beams each pass though a .0005 inch thick nickel foil which serves as a heat radiation barrier and as a beta filter for the copper x-radiation employed A xenon-

Table 1

Unit-cell parameters of high tridymite from the Steinbach
meteorite, as measured from precession photographs taken
at 220° C.

a = 8.74
b = 5.05
c = 8.24
V = 363.69 $Å^3$
Z = 8 SiO_2

filled proportional counter was used with pulse-height analysis to eliminate electrical noise and also the $\lambda/2$ and shorter wave-length harmonics.

Integrated intensities were collected by the normal fixed-counter, rotating-crystal method. The background was estimated by fixed-time counts at each end of the scan. Approximately 300 reflections were measured in all. This included all independent reflections within the range of the instrument, as well as about 125 additional reflections used to verify the proposed symmetry and to determine the precision of the measurements.

The data were corrected for Lorenz and polarization factors, for absorption by the crystal, and for absorption by the nickel-foil shield of the furnace. The programs used in this data reduction are described by Onken[5], except for the correction program for the nickel-foil shield, which was written by the author.

After correcting for these effects, the symmetry-related reflections were compared and found to show an average deviation of only 3.3% (in intensity, or F^2) from mmm symmetry. This corresponds to an average error of less than 2% in the structure factors; and so provides an excellent confirmation of the orthorhombic symmetry.

Determination and refinement of the structure

It was considered likely that the actual structure of the high form would be similar to the ideal high tridymite

structure proposed by Gibbs. In order to verify this a Patterson function was first calculated[5]. The positions of the maxima in the resulting maps confirmed the similarity of the general linkage of the ideal high-tridymite structure but showed that the atoms must be shifted from their ideal locations. The strong smearing of the silicon-oxygen and oxygen-oxygen maxima on the maps also showed that the oxygen atoms were strongly affected by thermal motion or disorder. The problem of the structure determination then became one of finding the directions and magnitudes of the distortion.

The transformation matrix relating the cell of the ideal hexagonal high-tridymite cell with the actual C-centered orthorhombic cell is $a_{ortho} = S\ a_{hex}$, where $S = 210/010/001$. The atom locations of the hexagonal cell may then be transformed to their "ideal" locations in the orthorhombic cell by $x_{ortho} = x_{hex}\ S^{-1}$. It should be noted that using this relationship between the two cells results in an interchange of the a and b axes of the orthorhombic cell relative to the cell given in International Tables. For this reason the equivalent positions of space group $C222_1$, in the orientation used in this study, are listed in Table 2.

The transformed locations of the atoms in the true space group are given in Table 3. It can be seen that, as mentioned above, there is one SiO_2 formula unit to be specified. The silicon atom and one of the oxygen atoms are in

Table 2

Coordinates of equivalent positions in space group $\underline{C}222_1$

for orientation used in this study.

Equivalent position	Symmetry	Coordinates
8 $\underline{c}$	1	x y z
		x, y z
		x y $\frac{1}{2}$ + z
		x y $\frac{1}{2}$ - z
		$\frac{1}{2}$ - x, $\frac{1}{2}$ + yz
		$\frac{1}{2}$ + x $\frac{1}{2}$ - y $\frac{1}{2}$ - z
		$\frac{1}{2}$ - x, $\frac{1}{2}$ + y, z
4 $\underline{b}$	2	0 y 0
		0 y $\frac{1}{2}$
		$\frac{1}{2}$ $\frac{1}{2}$ + y 0
		$\frac{1}{4}$ $\frac{1}{2}$ - y $\frac{1}{2}$
4 $\underline{a}$	2	x 0 $\frac{1}{4}$
		x 0 3/4
		$\frac{1}{2}$ + x, $\frac{1}{2}$, $\frac{1}{4}$
		$\frac{1}{2}$ - x, $\frac{1}{2}$ 3/4

Table 3

Coordinates of atoms in orthorhombic

cell as transformed from ideal hexagonal cell.

Atom	x	y	z
Si	1/6	1/2	7/16
O(1)	1/3	1/2	3/4
O(2)	0	1/2	1/2
O(3)	1/4	1/4	1/2

The symmetry-fixed parameters are underlined.

the general position. Two oxygen atoms occur in the special positions, $4\underline{a}$ and $4\underline{b}$, which are positions on two-fold axes.

A structure-factor calculation[5] was made using the values given in Table 3. The agreement between the observed and calculated structure amplitudes, in terms of the usual $\underline{R}$ factor was 42%. A least-squares refinement was then carried out of the positional and thermal parameters, in that order. The refinement converged to $\underline{R} = 13.4\%$, in five cycles. In the isotropic refinement the ratio of observation to variables is more than 13:1. As was expected, the apparent isotropic temperature factors of all the oxygen atoms were found to be very high, averaging about 7 $\overset{2}{R}$.

At this point an electron-density function and difference map were computed. The electron-density map clearly indicated that the oxygen atoms were elongated normal to direction of their bonds with the silicon atoms. Similarly, the difference map showed maxima corresponding to as much of 0.7 electrons near some of the oxygen-atom locations. With such evidence of anisotropic thermal motion, refinement was continued with anisotropic temperature factors. The restrictions to the thermal ellipsoids of the atoms lying on the two-fold axes is that, for $O(1)$, $\underline{B}_{12} = \underline{B}_{23} = 0$, and for $O(2)$, $B_{12} = B_{23} = 0$. The refinement converged in two cycles to $\underline{R} = 8.6\%$. In the case of anisotropic temperature factors the ratio of observations to variables is 6:1.

Another electron-density map and difference map were
then calculated. The electron-density map was essentially
identical with the previous one, showing that few, if any,
signs had changed in the anisotropic refinement. The
difference map, however, was quite changed from the pre-
vious map, and showed no anomalies near any of the atom
locations, indicating that the anisotropic thermal motion
was well described by the six-parameter ellipsoids.

Table 4 lists the final refined positional parameters
and their estimated standard deviations. Table 5 lists the
final refined thermal parameters in terms of the usual
anisotropic temperature factors, B_{ij}, and their estimated
standard deviations. A comparison of the observed struc-
ture amplitudes and those calculated from the final model
is given in Table 6.

A measure of the statistical significance of the dif-
ferences between the starting parameters of Table 3, and
the final parameters of Table 4 can be made by comparing
these differences with the final standard deviations. It
can be seen that the shifts amount to as much as forty
standard deviations, in the case of silicon.

Description of the structure

The final refined structure is illustrated in Figure 1.
Also shown are those symmetry elements of the orthorhombic
cell that are not hidden by the structure. In this view
the tetrahedra joined in the direction of the c axis are

Table 4

Final positional parameters of high tridymite at $\underline{R} = 8.6\%$

Atom	x	σ_x	y	σ_y	z	σ_z
Si	.16846	.00051	.53589	.00084	.43857	.00070
O(1)	.3336	.0031	0.	~	.75	~
O(2)	0	~	.5597	.0076	.5	~
O(3)	.2547	.0028	.3029	.0031	.5213	.0027

Table 5

Final thermal parameter at $\underline{R} = 8.6\%$

in term of the usual B_{ij} tensor.

Atom	B_{11}	σ	B_{22}	σ	B_{33}	σ	B_{12}	σ	B_{13}	σ	B_{23}	σ
Si	.0019A^2	.0006	.0260	.0016	.0119	.0013	.0012	.0010	-.0001	.0007	-.0013	.0009
O(1)	.040	.006	.080	.014	.017	.007	0	-	0	-	.009	.007
O(2)	.012	.002	.36	.023	.030	.007	0	-	.002	.003	0	-
O(3)	.041	.004	.054	.007	.025	.004	.024	.005	-.006	.003	.008	.005

Table 6

Comparison of observed and calculated structure amplitudes

hkl	F_o	F_c	hkl	F_o	F_c
2 0 0	26287	29155	7 1 0	7114	7452
0 2	22162	22170	4 4	3496	2887
4 0	1736	1815	1 5	1869	2259
6 0	16797	17118	7 3	2422	2796
0 4	11046	10872	8 2	2503	3775
8 0	3275	3022	6 4	4268	4552
10 0	1100	1207	3 5	3700	3865
0 6	2139	1823	9 1	4903	5605
2 0 1	16625	17044	5 5	917	1189
0 2	5156	5219	9 3	3003	3456
4 0	11505	10433	1 1 1	18074	17763
6 0	4942	211	3 1	3554	3090
0 4	13208	13862	2 2	12251	11445
8 0	3222	2986	5 1	9159	8156
1 1 0	27820	27746	1 3	10896	10757
3 1	22125	21786	4 2	9690	8530
2 2	945	1653	3 3	9626	9301
1 3	10844	10148	6 2	8436	6974
4 2	11566	10978	2 4	8009	8174
5 1	12112	12724	5 3	6419	6703
3 3	15604	15295	7 1	5366	4435
6 2	13737	14856	4 4	3050	2444
2 4	5374	5377	1 5	3318	3710
5 3	6116	6895	8 2	2496	2707

hkl	F_o	F_c	hkl	F_o	F_c
7 3 1	2809	2729	8 0 2	2955	1350
3 5	6012	5793	7 3	3178	3516
9 1	2860	941	1 5	4501	4736
6 4	4748	4633	8 2	2907	2918
5 5	1838	2485	3 5	2490	2158
10 0	1432	1778	9 1	3105	3408
0 6	4064	4751	6 4	2938	2663
9 3	2319	2245	5 5	3365	3380
1 1 2	14291	13605	10 0	1905	608
2 0	12964	12500	1 1 3	11520	11831
0 2	3917	4251	2 0	12378	12982
3 1	5263	5391	0 2	1490	1134
2 2	7709	6593	3 1	1565	1065
4 0	6874	6272	2 2	11954	11616
4 2	8038	7410	4 0	12431	12076
1 3	8163	7912	4 2	11279	10392
5 1	7348	7352	1 3	10995	10489
3 3	8289	7753	5 1	12120	10532
6 0	9395	9665	3 3	4067	3815
0 4	6155	5710	6 0	2548	471
6 2	8705	9290	0 4	5650	6537
5 3	6186	6056	6 2	3423	3300
2 4	6594	6301	5 3	5976	5601
7 1	5581	5158	2 4	6051	5585
4 4	4894	4924	7 1	7151	7496

hkl	F_o	F_c	hkl	F_o	F_c
4 4 3	4425	3471	7 1 4	3528	2148
8 0	6007	5578	4 4	5270	5622
7 3	3587	3902	8 0	2735	1070
1 5	2581	2169	7 3	3432	3660
8 2	3901	4204	1 5	4939	5440
3 5	2027	1866	8 2	2812	2026
9 1	1000	626	3 5	529	425
6 4	1712	1486	9 1	469	370
5 5	2012	2160	1 1 5	15033	14642
10 0	2715	3621	2 0	13771	15595
1 1 4	9404	9635	0 2	3685	3820
2 0	6476	4989	3 1	2254	1746
0 2	1954	830	2 2	12533	12767
3 1	3145	2725	4 0	12701	12305
2 2	7326	7034	4 2	10194	9991
4 0	5283	4650	1 3	10299	10454
4 2	5972	5581	5 1	10557	9753
1 3	7444	7658	3 3	3240	3246
5 1	4287	2295	6 0	1865	307
3 3	2173	2281	0 4	2496	1625
6 0	2049	1654	6 2	1503	1066
0 4	1507	2111	5 3	4638	4584
6 2	2012	2404	2 4	4607	4431
5 3	5348	5154	7 1	5953	6322
2 4	6503	6667	4 4	3697	3745

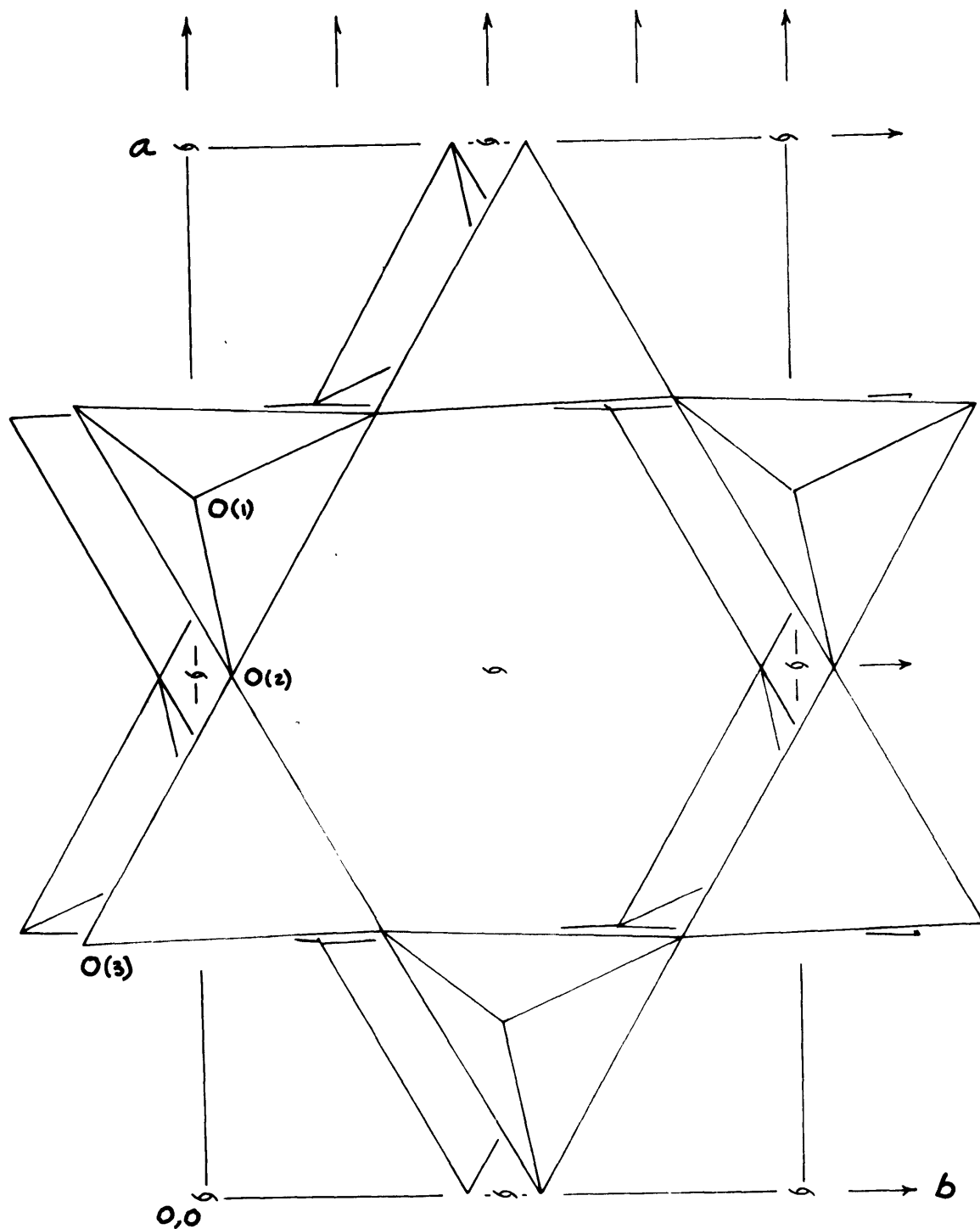| hkl	F_o	F_c	hkl	F_o	F_c
P 0 5	4778	4640			
7 3	2934	3219			
1 5	2421	2304			
8 2	3040	3535			
3 5	1965	2445			
9 1	964	762			
6 4	1703	1862			
1 1 6	6247	5920			
2 0	5058	5115			
0 2	10166	10202			
3 1	10585	10859			
2 2	5713	6783			
4 0	5725	6319			
4 2	3910	3274			
1 3	4212	3934			
5 1 6	3434	3164			
3 3	4459	4530			
6 0	5196	5374			
0 4	3444	2883			
6 2	4093	3531			
5 3	2514	2749			
2 4	3020	3218			
7 1	2032	1312			
4 4	2484	3163			
8 0	1775	2575			

Figure 1. Projection of orthorhombic high tridymite structure in c axis direction.

seen to be slightly offset from each other in the direction
of the b axis. This should be compared with the ideal struc-
ture where these same tetrahedra would project, in this
view, directly on top of one another. Figure 2 focuses atten-
tion on a smaller fragment of the structure as seen looking
along the a axis. In the ideal structure these tilted pairs
of tetrahedra would stand vertically along the c axis. The
observed tilt, relative to the c axis, amounts to about
8°. From the two figures it can be seen that the distor-
tion results in a slight flexure of joined tetrahedra at
O(2) and O(3), but that the tetrahedra joined at O(1) are
essentially as in ideal high tridymite.

Bond distances, bond angles, and their standard devia-
tions were computed using the program MGEOM[5]. The results
are listed in Table 7. In view of the large thermal motion,
the standard deviations are suprisingly low. The weighted
average Si-O distance in the tetrahedron, $\overline{d}_w = (\Sigma \frac{d_i}{c_i} / \frac{1}{c_i})$,
is 1.56 Å. This should be compared with the distances found
in quartz[7]; 1.603 and 1.616, and in low cristobalite[2];
1.601 and 1.608. The deviations of the individual bonds
from this weighted average is, in each case, less than one
standard deviation, implying that the tetrahedron is re-
gular in regard to distances.

The average of the tetrahedral angles listed in Table 7
is $109^\circ 27'$ which is almost exactly that of a regular tetra-
hedon. The deviations of the individual angles from the
average, however, are as much as four times the individual
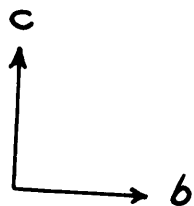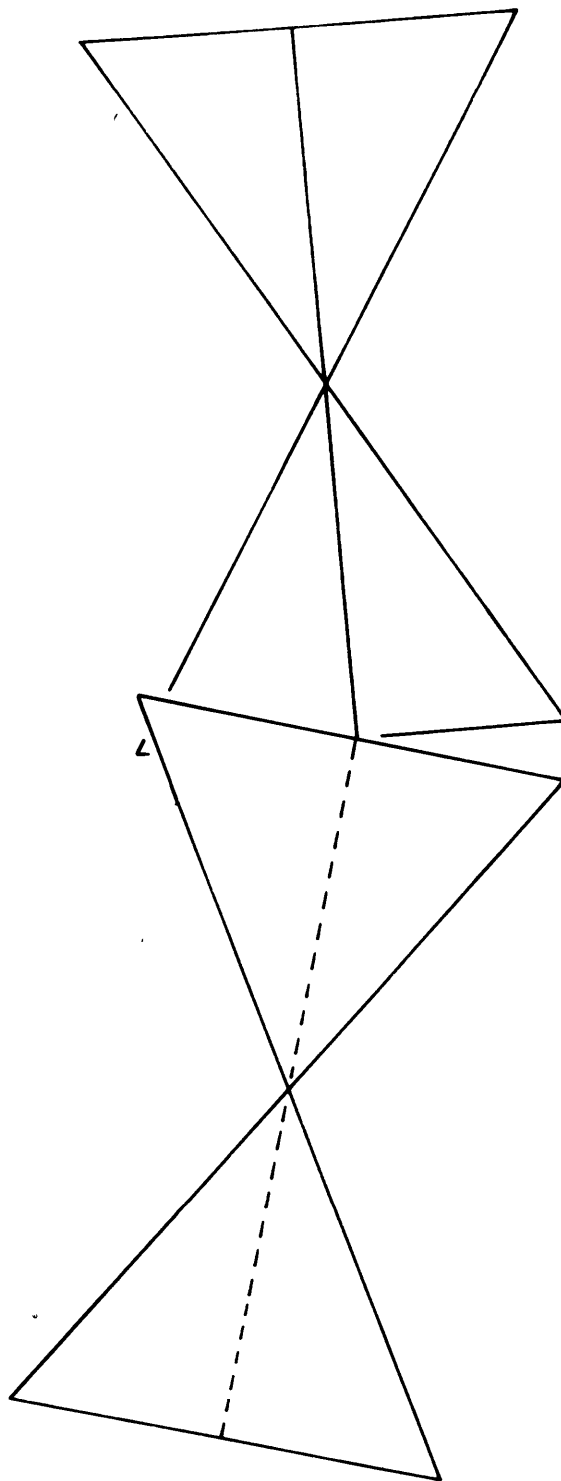
Figure 2. View of part of structure of high tridymite along
a-axis showing tilt of tetrahedra.

Table 7

Interatomic distances and angles in high tridymite

	Bond distances	σ
Si-O(1)	1.563 Å	.006 Å
Si-O(2)	1.561	.005
Si-O(3)	1.542	.017
Si-O(3')	1.554	.018

	Bond angles	σ
O(1)-Si-O(2)	108.7	1.4
O(1)-Si-O(3)	108.6	0.8
O(1)-Si-O(3')	11o.7	1.2
O(2)-Si-O(3)	105.9	0.8
O(2)-Si-O(3)	111.9	0.9
O(3)-Si-O(3')	110.0	1.5
Si-O(1)-Si	178.7	0.9
Si-O(2)-Si	171.2	2.7
Si-O(3)-Si	165.2	1.4

bond-angle standard deviations. This suggests that the tetrahedra do depart slightly from perfect regularity.

The Si-O-Si bond angles are all unequal. In the ideal high-tridymite structure these bonds are constrained by symmetry to be exactly 180°. In the actual structure the bond across O(1) does not depart significantly from this value. The bonds across O(2) and O(3), are significantly different from 180° and from each other, but both are still large compared to the "normal" values found in quartz[7], 143.5°, and in low cristobalite[2], 146.8°.

The anisotropic temperature-factor tensors were interpreted using the program THELOR[8]. Table 8 gives the root-mean-square amplitudes of thermal vibration in the directions of the principle axes of the thermal ellipsoids. The angles given are those between the respective principle axes and the crystallographic axes. The principle axis of the ellipsoid which most nearly parallels the crystallographic a axis is termed a' and so forth. For comparison the rms amplitudes found for quartz, at room temperature, are about .08 for Si and .09 to .14 for oxygen. The thermal ellipsoids given in Table 8 are shown plotted in Figure 3. It can be readily seen that the silicon atom is nearly spherical but that the oxygen atoms are highly elliptical. The most important point to notice is that the vibration amplitudes of the oxygen atoms normal to their bonds with the silicon atoms are almost twice that of their vibrations along the bonds.

Table 8

Root-mean-square amplitudes along principle axes of the
thermal ellipsoids, and orientation of ellipsoids with
respect to crystallographic axes.

Atom		rms amplitude	σ	angles (in°) between axes of ellipsoid and crystal		
				a	b	c
Si	a'	.215 Å	.005	8±10	14±6	9 ±14
	b'	.182	.006	96±5	12±8	80±9
	c'	.203	.011	85±14	100±9	11±9
O(1)	a'	.394	.028	0	90	90
	b'	.324	.27	90	11±11	80±11
	c'	.238	.047	90	101±11	11±11
O(2)	a'	.214	.021	3±6	90_	93+6
	b'	.419	.036	90_	0	90
	c'	.323	.035	87±6	90	3±6
O(3)	a'	.408	.015	16±4	75±4	96±5
	b'	.240	.018	106±4	27±9	111±11
	c'	.301	.024	91±5	68±10	22±10

Figure 3. Orientation and rms amplitudes of thermal

ellipsoids in SiO_4 tetrahedron of high tridymite, pro-

jected along b (top view), and c (lower view).
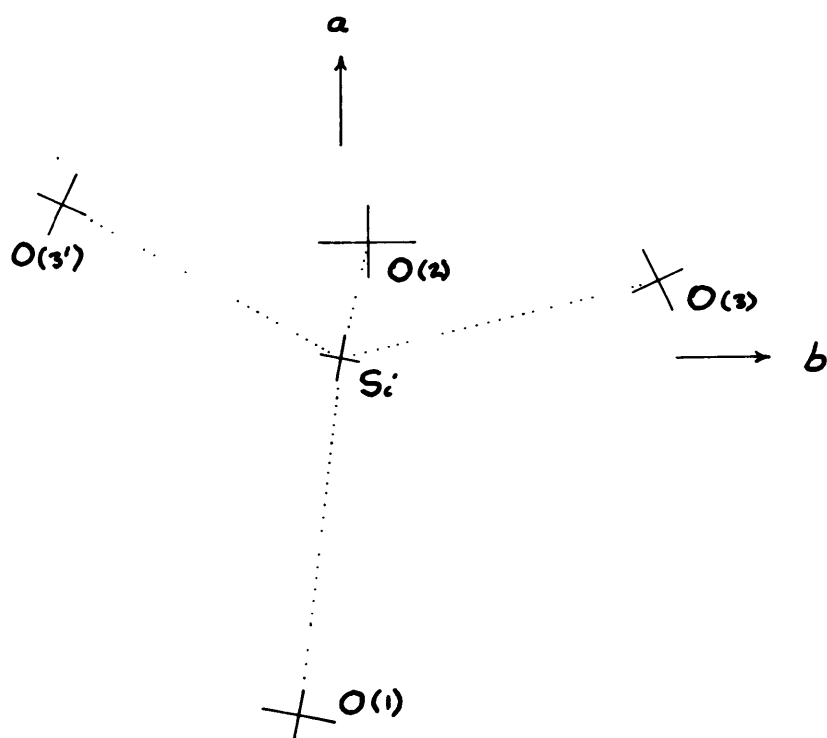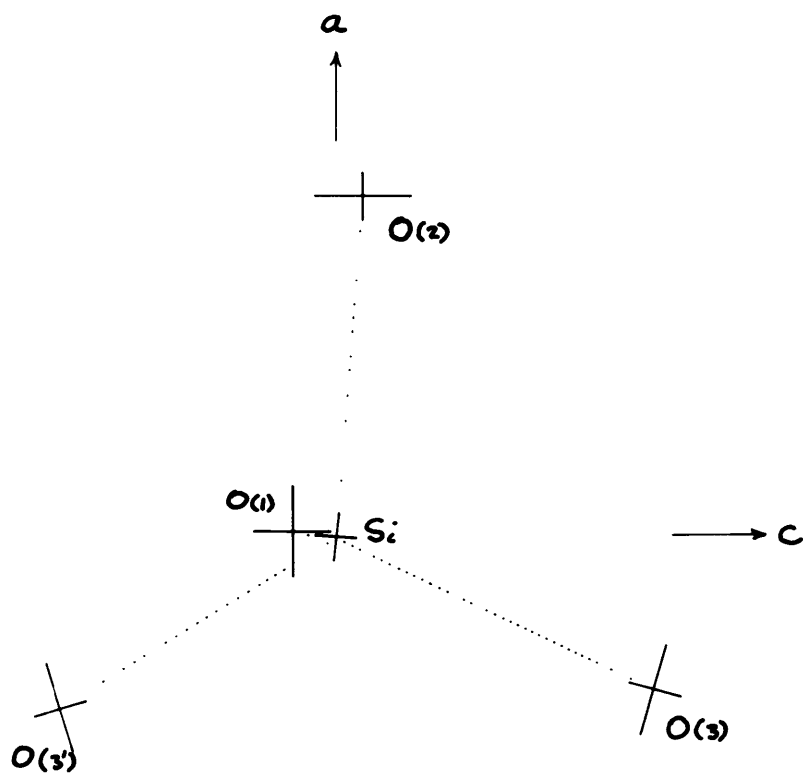
Figure 3.

The effect of this large-amplitude motion normal to the silicon oxygen bond is seen by considering the instantaneous position of the oxygen atom. If, for example, O(2) is considered as displaced from its time average position in the direction of the b axis, by its rms amplitude, the instantaneous Si-O(2) distance increases to 1.605 $\overset{o}{A}$ and the instantaneous Si-O(2)-Si angle decreases to about 156°. Both of the instantaneous values are close to those observed in room temperature structures. This model of thermal motion is somewhat similar to that proposed by Nieuwenkamp[9] for high cristobalite except that he considered the oxygen atom to be rotating about the circumference of a circle of radius .4 $\overset{o}{A}$.

Summary

In summary the true structure is seen to be distorted relative to the ideal high-tridymite structure. The distortion is a twisting of pairs of tetrahedra about the a axis such that tetrahedra joined in the c axis direction are alternately displaced in the plus and minus direction of the b axis. The amount of the twist is about 8° which causes the centers of the tetrahedra to be displaced by about 0.2 $\overset{o}{A}$. The atoms show strong thermal motion, and particularly the oxygen atoms in the directions normal to the silicon oxygen bonds. The tetrahedra are very nearly regular and the interatomic distances and angles are not too different from those reported for room temperature structures, provided the thermal motion is taken into account.

Acknowledgements

1. R. E. Gibbs, 1927, The polymorphism of silicon dioxide and the structure of tridymite, Proc. Roy. Soc. A., 113, pp. 351-68.

2. W. A. Dollase, 1966, Ph. D. Thesis.

3. Mitsuo Sato, 1964, X-ray study of tridymite (1) on tridymite M and tridymite S, Min. J. of Japan, 4, pp 115-130.

4. B. J. Wuensoh, 1964, Ph. D. Thesis.

5. H. H. Onken, 1964, Manual for some computer programs for ex-ray analysis.

6. International Tables for x-ray crystallography, 1952, vol. I, Symmetry groups, Int. Union of Cryst.

7. W. H. Zachoriasen and H. A. Plettinger, 1965, Extinction in quartz, Oct. Cryst. 18, pp. 710-714.

8. Allen C. Larson, R. B. Rosf, Jr., and Don T. Cromer, 1965, On integrated series of crystallographic computer programs, VIII Thermal ellipsoid orientation, Report La-3310 of the Los Alamos Scientific Laboratory.

9. W. Niewenkamp, 1937, Über die Structure von Hoch-Cristobalit, Zeit. Krist., 96, pp. 454-8.

Chapter VI

The crystal structure at 120° C of transitional tridymite from the Steinbach meteorite.

Abstract

Transitional tridymite is the phase of the Steinbach tridymite which exists between 107° C and 80° C and is characterized by a weak variable superstructure. The subcell of the phase is monoclinic $P2_1$ with $a = 5.04$, $b = 5.04$, $c = 8.23$ Å, and $\gamma = 120°$. The subcell reflections deviate only slightly from the orthorhombic $C222_1$ symmetry of high tridymite.

The refined structure is almost identical with that found for high tridymite at 220° C. The only definite deviations from the higher symmetry are very slight shifts of the silicon atoms in the $[1\bar{1}0]$ direction of the monoclinic cell. The apparent thermal motion is as large as that found in high tridymite although it is probably due in part to the regular deviations from the subcell positions which cause the superstructure.

Tridymite from the Steinbach meteorite has been shown in three previous chapters to exist in three distinct s'ructural states between room temperature and 250° C. The inter mediate-temperature phase, which is here termed transitional tridymite, occurs between about 107° C and about 180° C. This phase is characterized by the presence of a weak variable superstructure whose unusual behavior has been more fully described elsewhere. The supercell period of this weak superstructure varies between 65 Å and 105 Å over the temperature limits of this phase. Because of size of the supercell, and its variability with temperature, it was not considered feasible to collect the data or solve the complete (supercell) structure. Instead, in the nature of a preliminary investigation of the structure of this phase, this paper reports the averaged subcell structure of the transitional phase at 120° C.

Previous studies

In the temperature range under consideration (roughly $105 - 180^{\circ}$ C) no structural studies have been reported although a few papers have yielded structural implications and the presence of additional reflections has been noted. Buerger and Lukesh (1942) took Weissenberg photographs of two naturally occurring tridymites at temperatures just above their inversions from the low cells, and found, in addition to the reflections of high tridymite, a "pattern

of satellite reflections which varied in their distribution
in a definite manner with temperature". Hill and Roy (1958)
have schematically represented powder patterns of synthetic
tridymites taken at about 130° C which show additional lines
relative to both the room-temperature pattern and the pat-
tern of high tridymite. The behavior of reflections of a
natural tridymite were studied by Sato (1964) on a powder
diffractometer at temperatures up to 500° C. He noted the
essentially continuous change in both the shape and the in-
tensities of various reflections throughout the transitional-
temperature range and at least up to 260° C.

Unit cell and twinning

Precession photographs were taken of several crystals
of tridymite from the Steinbach meteorite at various temp-
eratures throughout the range of the transitional phase
using MoK and FeK radiation. The heating device employed
was similar to that constructed by Wuensch (1964). As
described previously, the subcell of the transitional phase
is dimensionally the same as the hexagonal high-tridymite
cell reported by Gibbs (1927). The symmetry is, however,
definitely lower and somewhat problematic. From films,
the substructure reflections taken by themselves seemed to
show orthorhombic symmetry. Later single-crystal diffracto-
meter measurements revealed slight deviations from this
apparent symmetry, as is described in detail below, and
showed the true symmetry of the subcell reflections to be

monoclinic. The dimensions of this monoclinic cell were
measured from the precession photographs, and the result-
ing parameters are listed in Table 1. There are thus four
SiO_2 formula-units per unit cell, as in ideal high tridy-
mite.

All the tridymites of this type that have been examined
have proved to be twinned. The twin law and a method of
determining the proportion of a grain in each of the twin
orientations have been given previously. The actual grain
used in the data collection was the same one used in the
room-temperature phase-data collection and was selected as
one of the most favorable grains found up to that time.
In the transitional phase this grain was determined to have
only 9.6% of its volume in twinned orientation relative to
the main part of the grain. Because of this small value,
and larger errors from other sources, the small effect of
this twinning on the reflection intensities could be ignored.

Determination of the symmetry

In order to determine the true symmetry of the trans-
itional phase, the intensities of a large number of reflec-
tions from several different crystals were measured at var-
ious temperatures between 20° C to 250° C on a single-crystal
counter diffractometer. The behavior of the transitional-
phase satellites has already been described (see Chapter 4).
The substructure reflections were also noted to change in
intensity in this region, as had been reported by Sato, but

Table 1

Subcell parameters at 120° C of tridymite

from the Steinbach meteorite

$$a = 504 \text{ Å} \qquad \alpha = 90^{\circ}$$
$$b = 5.04 \qquad \beta = 90^{\circ}$$
$$c = 8.23 \qquad \gamma = 120^{\circ}$$

the magnitude of the changes are not nearly as drastic as
those of the supercell reflections. Typically, the subcell
reflections were observed to have their maximum value at a
temperature just above the transition from the low-tempera-
ture form, and to decrease in intensity, more-or-less con-
tinuously, throughout the transitional-phase temperature
range. Near the transition of the high phase the changes
were seen to level off to the normal slow decrease of in-
tensity with temperature that is expected.

Examination of the intensity measurements made just
above the transition from the low-temperature form suggested
that the symmetry at this temperature was monoclinic. Pre-
vious studies had shown that above 180° C the symmetry was
orthorhombic. Thus it would appear that the observed in-
tensity changes are involved with this symmetry change, and
that certain pairs of reflections which are unequal in inten-
sity at about 110°, must converge to equal intensity by
about 180° C. This indicated behavior was then confirmed
on the diffractometer by following pairs of equivalent
reflections as the temperature was decreased from the high
form, and noting a slight but real divergence in many of
the cases.

Accepting the symmetry then as monoclinic, the diffrac-
tion symbol was determined to be $2/mP2_1/-$. The space group
must therefore be $P2_1/m$ if the crystal is centrosymmetric
but $P2_1$ if it is noncentric. In the former case there would

be one formula unit of SiO_2 in the asymmetric unit of the space group, and in the latter case, there would be two formula units.

Data collection and correction

The intensities of the substructure reflections were then measured on the single-crystal diffractometer out to $sin \theta/\lambda = 0.4$. The procedures employed were the same as have been previously described except that molybdenum radiation was used with NaI(Tl) scintillation counter. About two hundred independent reflections were collected. For control, a few reflections were remeasured a number of times during the course of the data collection to ensure a constancy of conditions. The reflections were corrected for Lorenz and polarization factors. Absorption of the molybdenum radiation by the crystal was negligible.

Determination and refinement of the structure

A three-dimensional Patterson function was computed. For the space group $\underline{P2_1/m}$, the Patterson map has a Harker line at $00\underline{z}$, and a Harker section at $\underline{xy\frac{1}{2}}$. (See Buerger, 1959) Since there would be only one independent silicon atom in this space group, this Harker line should contain a silicon-silicon peak. If, alternatively, the symmetry is $\underline{P2_1}$, there must be two independent silicon atoms in the cell, and these need not, in general, give rise to a peak at $00\underline{z}$ in the Patterson map; the Harker section should,

in general, show two separate silicon-silicon peaks.

Examination of the Patterson map showed peaks of appropriate height for silicon-silicon peaks: one of these occurred near, but definitely off, the line 00z, and two such well resolved peaks occurred in the Harker section. The space group is therefore $\underline{P2}_1$.

Trial locations for the two silicon atoms were taken from the Patterson map and used to calculate structure factors. The agreement between observed and calculated structure factors, in terms of the unual $\underline{R}$ factor was 34%. An electron-density map was then computed using the phases determined by the two silicon atoms. The resulting map showed the locations of the oxygen atoms, but also showed that these atoms were highly smeared out.

Starting with the parameters obtained from the electron-density map, and employing isotropic temperature factors, the structure was refined to $\underline{R}$ 11.7%. The ratio of observations per variable was 8:1. The final refined positional and thermal parameters are given in Table 2. The comparison of observed and calculated structure amplitudes is given in Table 3.

As was expected from the electron-density map, the refined oxygen-atom temperature factors are very high. The apparent magnitude of the thermal vibrations could probably be decreased by continued refinement with anisotropic temperature factors. In this case, however, such refinement is not warranted. The ratio of observations per variable

Table 2

Final refined positional and thermal parameters of
transitional tridymite at 120° C.

Atom	x	σ_x	y	σ_y	z	σ_z	B	σ_B
Si(1)	.2988	.0021	.6153	.0021	.0632	.0017	2.3$\mathring{A}^2$	0.2
Si(2)	.3719	.0021	.7245	.0021	.4389	.0017	2.5	0.2
O(1)	.3361	.0079	.6788	.0087	.24[*]	-	5.9	0.7
O(2)	.4399	.0090	.4081	.0085	.0129	.0082	9.3	1.0
O(3)	.9326	.0092	.4046	.0036	.0214	.0085	9.8	1.0
O(4)	.5579	.0070	.0692	.0068	.4634	.0075	5.7	0.7

[*] arbitrarily set to determine origin

Table 3

Comparison of observed and calculated structure amplitudes

h	k	l	F_o	F_c	h	k	l	F_o	F_c
0	0	2	13103	14206	3	0	5	1165	1100
0		4	6196	5801	3		6	1630	1757
0		6	4166	4210	3		7	1541	1500
0		8	2991	2762	4		0	2128	1225
-1		0	10202	10403	4		1	1157	941
-1		1	6698	6287	4		2	1479	1651
1		2	5084	5151	4		3	1239	1326
-1		3	3899	3842	4		4	1782	1753
-1		4	3315	3367	-1	1	0	11377	10884
1		5	5116	4969	-1		1	7241	6330
-1		6	3370	2874	-1		2	4928	4717
1		8	1470	1483	-1		3	4223	4415
2		0	662	728	-1		4	2421	2651
2		1	4050	4235	-1		5	5336	5661
2		2	2695	2462	-1		6	2579	2396
2		3	3825	3995	-2		0	8949	8918
2		4	2664	2452	0		1	7349	6694
2		5	4272	4153	-2		1	1007	963
2		6	2065	2353	0		2	5810	5596
3		0	4627	5039	-2		2	2562	2766
3		1	3247	3094	0		3	3576	3893
3		2	2429	2335	-2		3	592	581
3		3	1610	1252	0		4	4493	4827
3		4	797	561	-2		4	1411	1832

h k l	F_o	F_c		h k l	F_o	F_c
0 1 5	4922	5188		-4 1 2	2193	1797
-2 5	835	440		2 33	3603	3725
0 6	3548	2854		-4 3	1933	1891
-2 6	4195	4523		2 4	2940	2692
0 7	1022	643		-4 4	1675	1500
-2 7	759	493		2 5	3474	3588
1 0	7998	8104		3 0	1455	1402
-3 0	4613	4396		3 1	2845	2853
1 1	2389	2402		3 2	2205	2130
-3 1	3335	3517		3 3	1895	1805
1 2	1696	1563		3 4	2421	2386
-3 2	2855	2972		-3 2 1	3349	3335
1 3	857	691		-2 1	900	177
-3 3	3802	3820		-2 1	4555	4192
1 4	819	895		-2 2	2693	2329
-3 4	2090	2007		-2 3	4236	4161
1 5	1590	1406		-2 4	2207	4120
-3 5	3795	3527		-2 5	4558	4808
1 6	3639	3670		-2 6	2255	2307
1 7	1605	1620		-3 0	4929	5069
2 0	3191	3078		-2 1	1945	1957
-4 0	2004	2121		-1 2	1670	1727
2 1	3798	3861		-3 2	2825	2727
-4 1	1812	2041		-1 3	851	923
2 2	2795	2716		-3 3	4302	4367

h	k	l	F_o	F_c	h	k	l	F_o	F_c
-1	2	4	1175	1133	2	2	2	1262	853
-3		4	1483	1128	2		3	2172	2226
-1		5	1556	1307	-3		0	6126	6281
-3		5	4128	4176	-3	3	1	2131	2054
-1		6	3854	4052	-3		2	3259	2911
-3		6	1416	1463	-3		3	1344	1082
0		0	1071	1401	-3		4	768	480
-4		0	5271	5843	-3		5	743	584
0		1	4688	4187	-3		6	1988	2459
-4		1	2166	1806	-2		0	3576	4190
0		2	3544	3087	-4		0	2878	2710
-4		2	3025	3417	-2		1	3568	3792
0		3	3809	3882	-4		1	1739	1908
-4		3	1029	855	-2		2	2479	2411
0		4	3846	3399	-4		2	2100	1573
0		5	4386	4596	-2		3	3956	3829
0		6	2345	2258	-4		3	2567	2756
1		0	3404	3099	-2		4	2198	2078
1		1	4083	4054	-4		4	1196	559
1		2	3210	3238	-2		5	3843	3679
1		3	3205	3093	-4		5	2245	2575
1		4	3549	3653	-2		6	1471	1461
1		5	3330	3297	-4		6	883	761
1		6	1910	1982	-1		0	3095	3728
2		0	2780	2489	-5		0	1252	1510

h	k	l	F_o	F_c
-1	3	1	3753	3626
	-5	1	1054	1306
	-1	2	2743	2946
	-5	2	962	902
	-1	3	3251	3127
	-1	5	3337	3313
	-1	5	3490	3662
	-1	6	1852	1624
	0	0	4165	4270
	0	1	4505	4824
	0	2	1947	1475
	0	3	2185	1888
	0	5	1393	1602
	0	6	1455	1593
	1	0	825	467
	1	1	3212	3059
	1	2	2493	2529
	1	3	1729	1614
	1	4	2934	2940
	1	5	956	1021
	1	6	1377	1333
	2	0	0	921
	2	1	1169	1349
	2	2	1704	1900
-4	4	0	3047	1502

h	k	l	F_o	F_c
-4	4	1	1222	1293
	-4	2	1283	1199
	-4	3	2250	2009
	-3	0	2408	2370
	-3	1	2998	2571
	-3	2	2190	1830
	-3	3	2538	2464
	-3	4	2121	1844
	-2	1	3520	4395
	-2	2	1560	2022
	-2	3	2021	1969
	-2	4	446	626
	-1	0	921	1166
	-1	1	3077	3027
	-1	2	2574	2482
	-1	3	1749	1787
	-1	4	3113	2993
	0	0	2038	1278
	0	1	1255	1335
	0	2	2185	2357
	0	3	479	213

would drop to only 3½:1, which begins to allow errors in the dat to be absorbed by the refinement. In addition, anisotropic thermal motion is probably not, in itself, the cause of these high values, as is discussed below.

A final electron-density map was computed after the refinement. The oxygen atoms could be seen to be definitly elongated in the directions normal to their bonds with silicon atoms.

Interpretation of the refinement model

<u>Positional parameters</u>. As was noted above, the substructure reflections of the transitional phase show only relatively small deviations from othorhombic symmetry. The first test of the validity of the refinement is therefore whether or not the refined structure deviates significantly, in a statistical sense, from the symmetry of the orthorhombic high phase.

In passing from monoclinic symmetry to the orthorhombic symmetry of the high phase Si(1) becomes equivalent to Si(2), O(3) becomes equivalent to O(4), and O(1), and O(2) are required to move to special positions on the two-fold axes. Table 4 lists in the first column the deviation of these pairs of atoms from such equivalence, or for the case of the single atoms, the deviation from such special position. The second column lists the standard deviations of the parameters as determined from the monoclinic refinement. The last column gives the magnitudes of the deviations from

Table 4

Statistical significance of deviations of transitional tridymite from high tridymite, based upon the present refinement.

Atom	orthorhombic coordinate	deviation from $C222_1$	standard deviation	significance
Si(1,2)	x	.018 Å	.002 Å	9
	y	.004	.002	2
	z	.002	.001	2
O(3,4)	x	.020	.008	2.5
	y	.018	.008	2.3
	z	.015	.008	1.9
O(1)	x	-	-	-
	y	.007	.009	0.8
	z*	-	-	-
O(2)	x	.016	.009	1.8
	y	-	-	-
	z	.013	.008	1.6

* This parameter is taken as origin-determining, and may be set arbitrarily.

orthorhombic symmetry in the form of the number of standard deviations of this parameter. It can be seen that on the basis of this refinement, the only atoms which deviate significantly from the symmetry of the high phase, are the silicon atoms.

The significance of the deviations of the silicon atoms indicate that these atoms are in different positions in the two phases. The non-significance of the oxygen-atom shifts does not imply that these atoms have identical positions in the two phases, but merely means that the refinement has not furnished any meaningful evidence of a difference in position.

Figure 1 shows the refined positions of the atoms in the monoclinic unit cell. As could be expected from the above remarks, this figure is almost identical with the corresponding view of the high-tridymite structure illustrated in that paper. The interatomic distances and angles were calculated from the refined positions and are listed in Table 5.

The average Si-O tetrahedral distance is 1.56 $\overset{\circ}{A}$, the same value found in high tridymite at 220° C. The range of distances is only slightly more than one standard deviation. The tetrahedral angles also do not depart significantly from those of a regular tetrahedron. Finally, the silicon-oxygen-silicon bond angles are within one or two standard deviations of the same values found in high tridymite at 220° C.

Table 5

Interatomic distances and angles in transitional tridymite
at 120° C.

Si(1)-O(1)	1.59 Å
Si(1)-O(2)	1.58
Si(1)-O(3)	1.54
Si(1)-O(4)	1.60
Si(2)-O(1)	1.53
Si(2)-O(2)	1.52
Si(2)-O(3)	1.58
Si(2)-O(4)	1.57
e. s. d. (Si-O)	.03 Å
O(1)-Si(1)-O(2)	107.6°
O(1)-Si(1)-O(3)	108.3
O(1)-Si(1)-O(4)	112.7
O(2)-Si(1)-O(3)	108.4
O(2)-Si(1)-O(4)	110.7
O(3)-Si(1)-O(4)	109.0
O(1)-Si(2)-O(2)	111.2
O(1)-Si(2)-O(3)	110.6
O(1)-Si(2)-O(4)	108.3
O(2)-Si(2)-O(3)	108.4
O(2)-Si(2)-O(4)	108.0
O(3)-Si(2)-O(4)	110.3
e. s. d. (O-Si-O)	1 - 2°
Si(1)-O(1)-Si(2)	178.0°
Si(1)-O(2)-Si(2)	168.5
Si(1)-O(3)-Si(2)	164.2
Si(1)-O(4)-Si(2)	167.8
e. s. d. (Si-O-Si)	2 - 3°
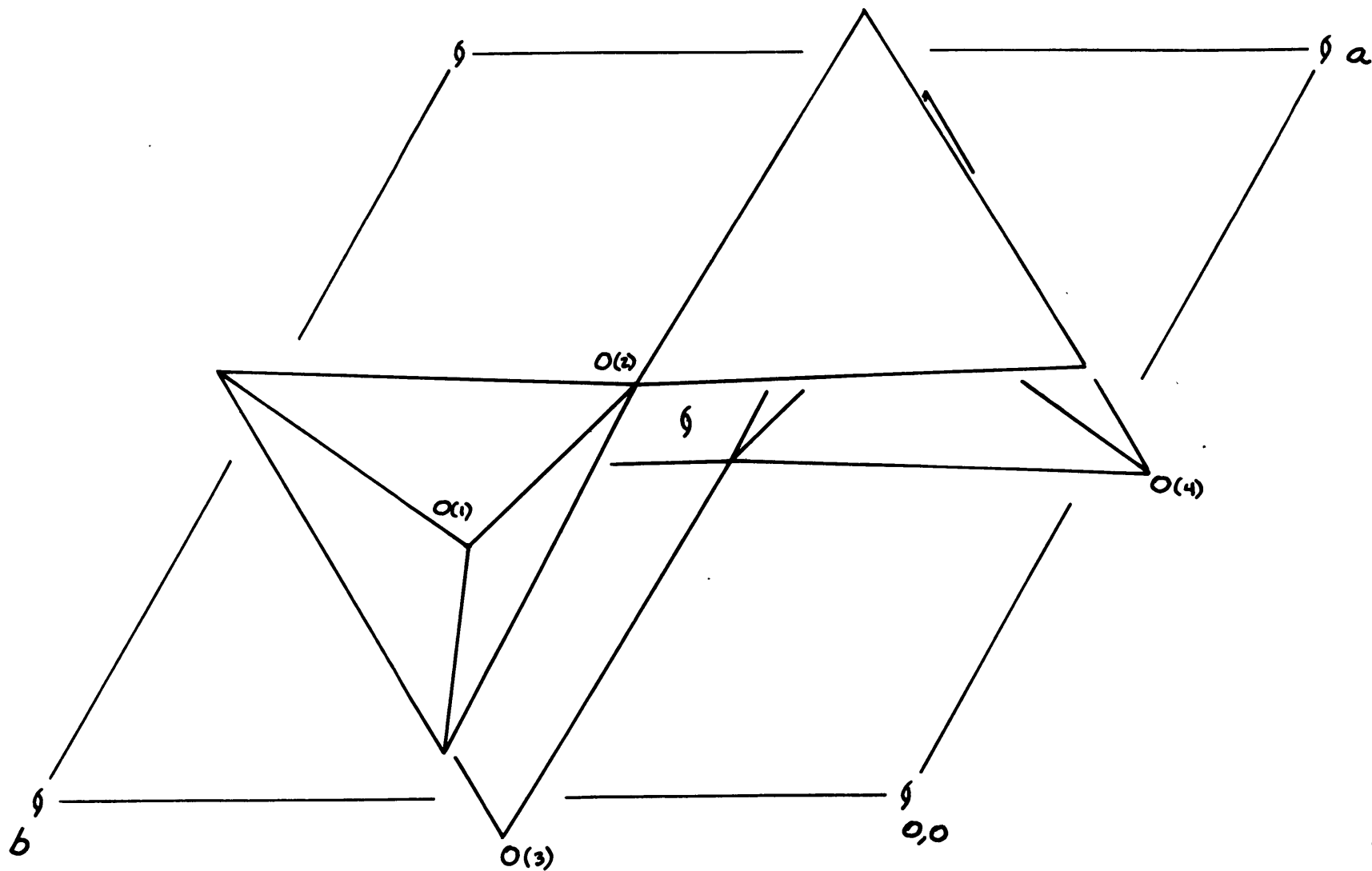
Figure 1. Projection of transitional tridymite along c axis.

Thermal parameters. Due to the overall similarity
of the transitional-phase structure with that of the struc-
ture of the high-temperature phase similar large amplitude
thermal vibration is expectable. The observations of elon-
gated atoms in the electron-density maps and large isotropic
temperature factors may then be interpreted in the same
way as in the structure of the high-temperature phase (see
previous chapter). There is, however, a contributing fac-
tor to the apparent thermal motion in the case of transi-
tional tridymite. This is due to the fact that only the
substructure reflections of the transitional-phase super-
structure were considered. The refined model thus repre-
sents the averaged structure, and any deviation of an atom
from the averaged position appears in the form of a larger
temperature factor for that atom (in the refinement model)
or as an elongated atom (in the electron-density maps).
The actual observations then probably represent a combina-
tion of true thermal motion and small deviations of the atoms
from their subcell averaged position. Such small, ordered,
deviations from the subcell average position would be in
keeping with the model proposed in Chapter 4 to explain
the dynamic superstructure.

Summary

The symmetry of the transitional-tridymite subcell at
$120°$ C is monoclinic, $\underline{P2_1}$. The substructure reflections

deviate only slightly from orthorhombic $C222_1$ symmetry.
The average positions of the atoms in the subcell, as deter-
mined by a least-squares refinement, do not deviate signif-
icantly from $C222_1$ symmetry, except in the case of the
silicon atoms. The refinement shows that the two-fold axes
of the high-tridymite orthorhombic cell are lost in the
transformation to the transitional phase. The change of
the structure appears to be a very slight twist of the tetra-
hedra about the c axis, but shifts in the positions of cor-
ners of the tetrahedra (the oxygen atoms) could not be proved
from the refinement. The observed thermal-vibration ampli-
tudes seem to be similar to those found in high tridymite
at 220° C, and are doubtlessly augmented by the (ordered)
atomic displacements from the subcell positions which give
rise to the transitional-phase superstructure.

M. J. Buerger and J. Lukesh, 1942, The tridymite problem, Sci. 95, pp. 20-21.

M. J. Buerger, 1959, Vector Space, John Wiley and Sons, New York, New York.

V. G. Hill and Rustum Roy, 1958, Silica structure studies VI on tridymite, Trans. Brit. Ceram. Cos. 57 pp. 496-510.

Mitsuo Sato, 1964, X-ray study of low tridymite (2) structure of low tridymite, type M, Min J. of Japan, 4, pp. 131-46.

B. J. Wuensch, 1964, Ph. D. Thesis, M.I.T.

Appendix

An improved furnace for use with a single-crystal
counter diffractometer.

The heating attachment employed in most of the single-crystal diffractometer measurements was expressly designed for this tudy and has proved to be quite useful. Since it has not been described elsewhere, this appendix provides the details of its design and construction necessary to allow a copy to be made, if desired. Figures 1-4 are reproductions of the actual workin drawings from which the furnace was constructed at the Electronics Systems Laboratory, at M.I.T.

The design of the furnace was based largely upon similar designs by M. J. Buerger, N. W. Buerger, and others, although their instruments were constructed for film studies at high temperatures. Prior to the construction of the furnace described below, initial film and diffractometer studies were made by the author using a heating device of the type described by Wuensch. The drawbacks of this type of furnace, and the experience gained in its use, influenced the design of the new furnace.

Design

For use with a single-crystal counter diffractometer a heating attachment should ideally satisfy the following

major requirements; for a given setting, the temperature
in the furnace should remain constant indefinitely, the
heating attachment should not decrease the volume of re-
ciprocal space which may be explored by the diffractometer,
and the temperature should be variable continuously from
room temperature to the melting point of the substance under
investigation. Subsidiary requirements of the ideal heat-
ing attachment are that it shoud allow the crystal to be
reoriented at high temperatures and that any absorption of
the x-ray beam by the diffractometer, be of a correctable
form.

The final practical design must, of course, be a com-
promise between the several desired characteristics, and
in addition, depends upon the materials available, the
space available on the diffractometer, the cost, etc. It
was found that, by choosing the desired diffraction geo-
metry and be optimizing the most desired characteristics,
the design was essentially fixed.

The equi-inclination geometry of data collection was
considered preferrable since it allowed all of reciprocal
space (out to a certain limit) to be explored without re-
mounting the crystal, and since it led to a simple correc-
tion for absorption by the furnace. In order to maintain
the temperature constant it was decided that the furnace
should be as enclosed as possible. The only opening need
be that required to admit the crystal and its supporting

glass fiber. In order to support the enclosure as well as the heating element itself it was necessary to restrict the angular range of the diffractometer. The furnace was then designed to allow a maximum equi-inclination angle of $45°$.

Materials and construction

The individual components of the furnace are numbered in the working drawings shown in Figures 1-4. The heating element is a coil of resistance wire which is allowed to expand within the supports (1) and (2). These supports are fired pyrophylite turnings, which should withstand a furnace temperature of $1000°$ C. The heating element and its supports slide into a cyclindrical brass cartridge (3) and are held in place by caps (4) and (5). One end of the heating coil is grounded to the cartridge, and the other end is passed through the body of support (1), to a screw threaded into the end serving as a binding post.

The cartridge is wrapped with a single layer of nickel foil .0005-inches thick which serves as the furnace enclosure. The foil easily passes copper or molybdenum x-radiation but forms a barrier to the escape of heat radiation. The wrapped cartridge is inserted into the furnace cooling jacket (6) and held in place by the cap (7). The water cooling jacket (6) is constructed of two coaxial brass cyclinders that have been heat-fitted and silver-soldered together at the ends. The channels through which the cooling

water circulates are cut into the cylinders prior to their being joined. The water jacket (6) is silver-soldered to the support arm (9) which is a bent brass bar held in place on the diffractometer by means of an aluminum dovetail assembly (10), (11) and (12). The dovetail is attached with screws to the crystal-rotation-axis support of the diffractometer.

With the crystal in place, the support arm of the assembled furnace is inserted into the dovetail, and the furnace is drawn into place over the crystal. The electrical contacts are made to the heating coil through the contact post screwed into (1), and through the grounder furnace support. The temperature is controlled by varying the voltage across the heating coil by means of a Variac. The total energy consumed by the heating coil is measured by a wattmeter whose reading is used to determine the furnace temperature from a calibration curve. This curve must be established by thermocouple and known melting-point measurements.

Figure 1.

Section (No exterior Detail)
Shown

45° Bevel

13/16
OVERSIZE

5/8

1 5/8

7/32

¢

3/8

1/4

5/8

1 5/16

drill & tap 1/4 deep
to fit ⑥

Knurl ⑦

1/2

25/32

9/16

3/16

45° bevel

1 1/16
threaded

1 5/16   O.D.

3/4

3/16

¢

⑥

Figure 2.

122

$11\frac{3}{4}$

$\frac{9}{16}$

$1\frac{7}{32}$

not critical

Dovetail cut to extend $3\frac{1}{2}"$

+

⑨

$1\frac{11}{32}$

45°

+

$\frac{1}{8}$

$\frac{5}{16}$

45°

$\frac{1}{4}$

1
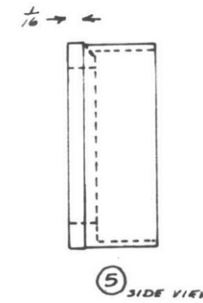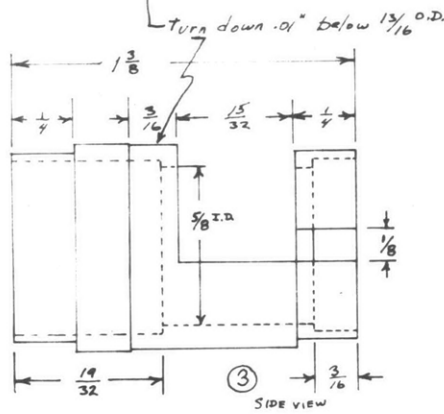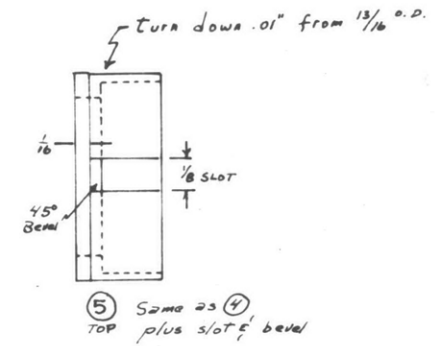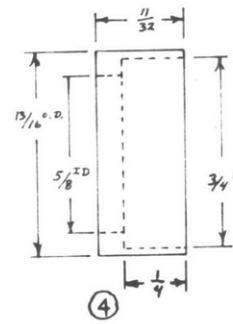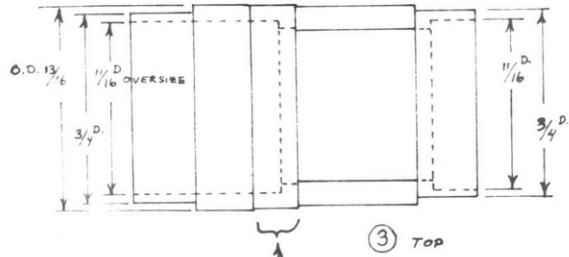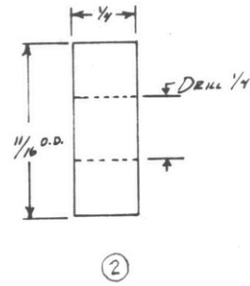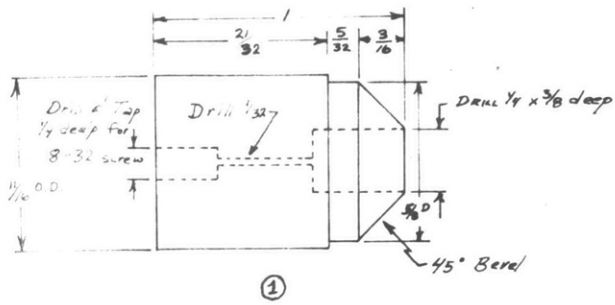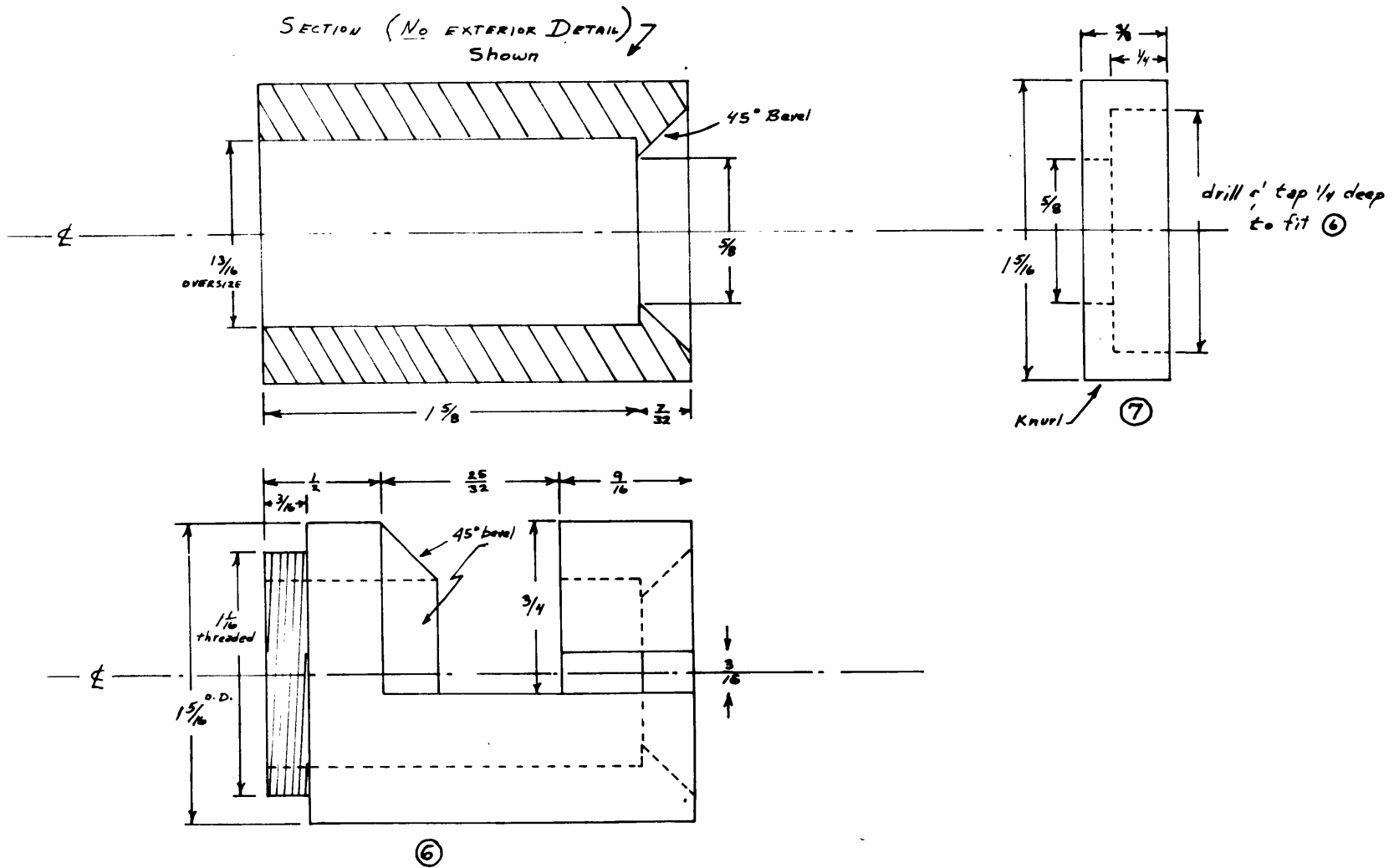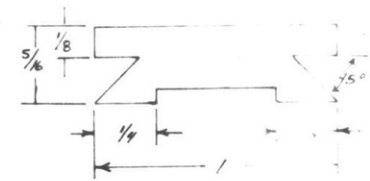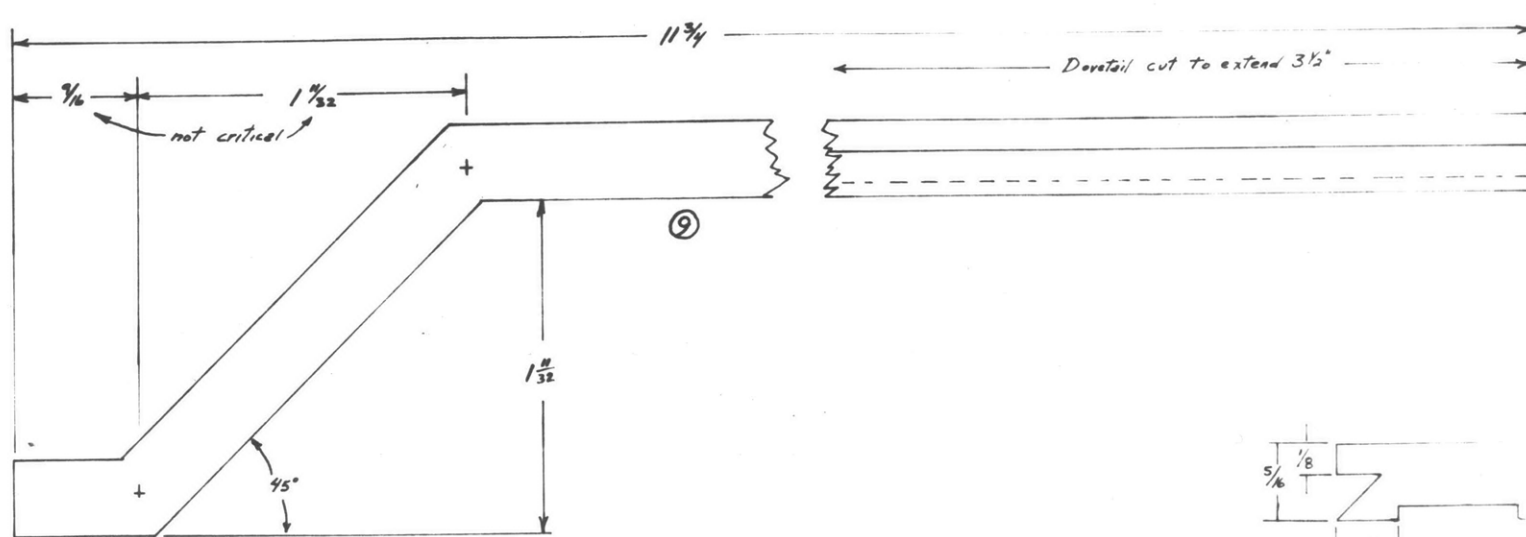
Right end view
with dovetail detail

$\sim 2\frac{1}{32}\,^R$ (to fit ⑥)

Left end view
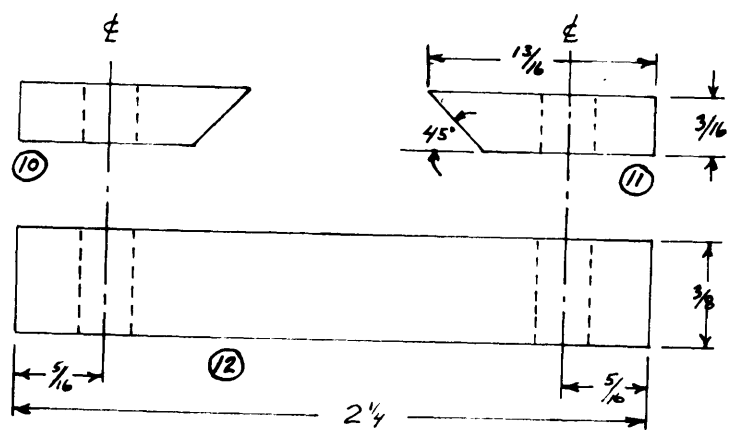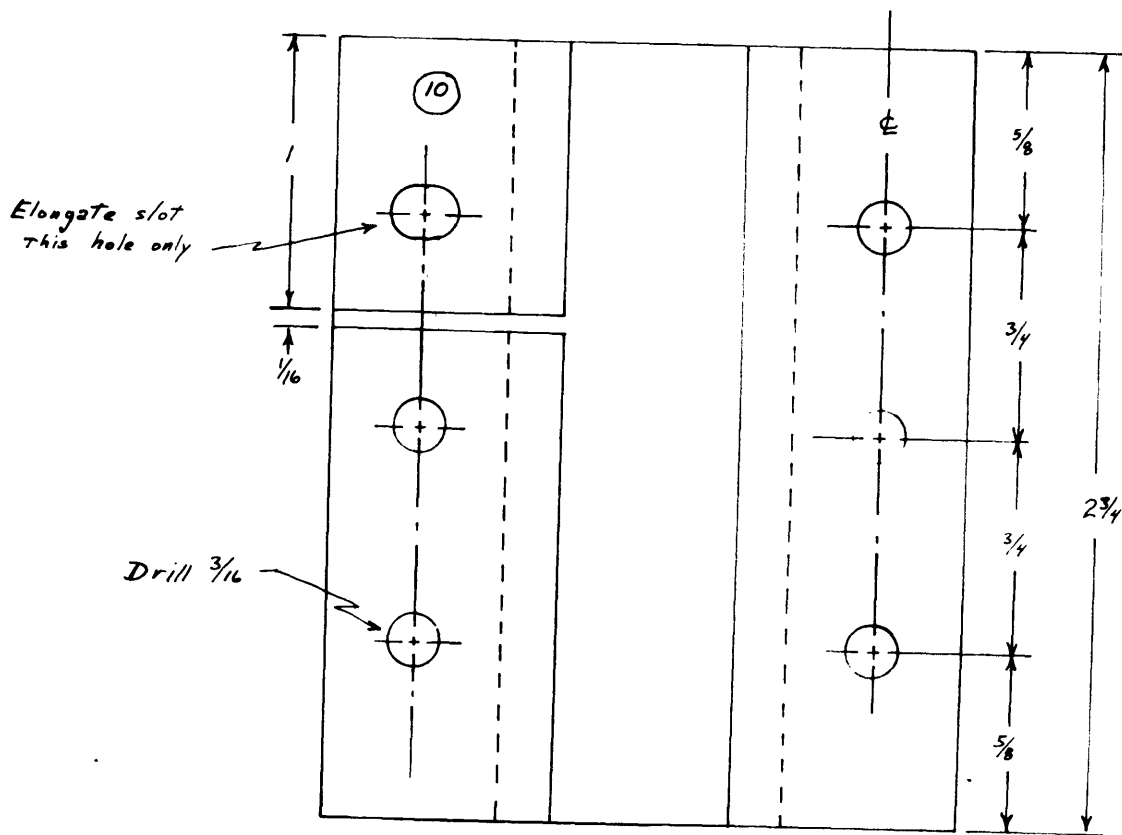
Figure 3.

Elongate slot
This hole only

Drill 3/16
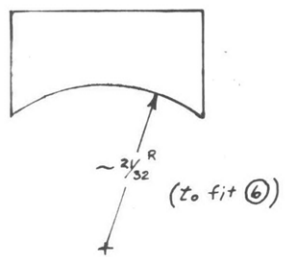
Figure 4.

M. J. Buerger, Newton W. Buerger, and Frank G. Chesley, 1943, Apparatus for making x-ray powder photographs at controlled, elevated temperatures, Am. Min., 28, pp. 285-302.

Newton W. Buerger, 1941, The chalcoeite problem, Econ. Geol., 36, pp. 19-44.

Newton W. Buerger, 1941, Weissenberg controlled-temperature technique, Am. Min., Abs. of 22nd M. S. A. meeting.

B. J. Wuensch, 1964, Ph. D. Thesis, M.I.T.

Biography

The author was born in West Bend, Wisconsin on August 16, 1938 and attended primary and secondary schools in West Bend and Watertown, Wisconsin. He attended the University of Wisconsin at Madison from 1956 to 1961 receiving the degree of Bachelor of Science with Senior Honors, in June 1960 and the degree of Master of Science (Geology) in August 1961.

From September 1961 to June 1966 he has been enrolled in a Ph. D. program at the Massachusetts Institute of Technology.

The author is a member of the American Crystallographic Association, the Mineralogical Society of America, and the American Association for the Advancement of Science. The author's previous publications are listed on the following page.

Publications of Wayne A. Dollase

1. The crystal structure and molecular structure of dibenzene-chromium. (with F. A. Cotton and J. S. Wood), J. Am. Chem. Soc. 85 (1963) 1543-1544.

2. The metal metal bonded, polynuclear complex anion in CsReCl$_4$. (with J. A. Bertrand and F. A. Cotton), J. Am. Chem. Soc. 85 (1963) 1349-1350.

3. The crystal structure of cesium dodecachloratrirhenate (III), a compound with a new type of metal atom cluster. (with J. A. Bertrand, F. A. Cotton), Inorganic Chemistry 2 (1963) 1166-1171.

4. Shape of the recorded area in precession photographs and its application in orienting crystals. (with M. J. Buerger), Science 145 (1964) 264-265.

5. The crystal structure of tetracyano-1,4-dithiin, J. Am. Chem. Soc. 87 (1965) 979-982.

6. Reinvestigation of the structure of low cristobalite. Z. Kristallogr. 121 (1965) 369-377.